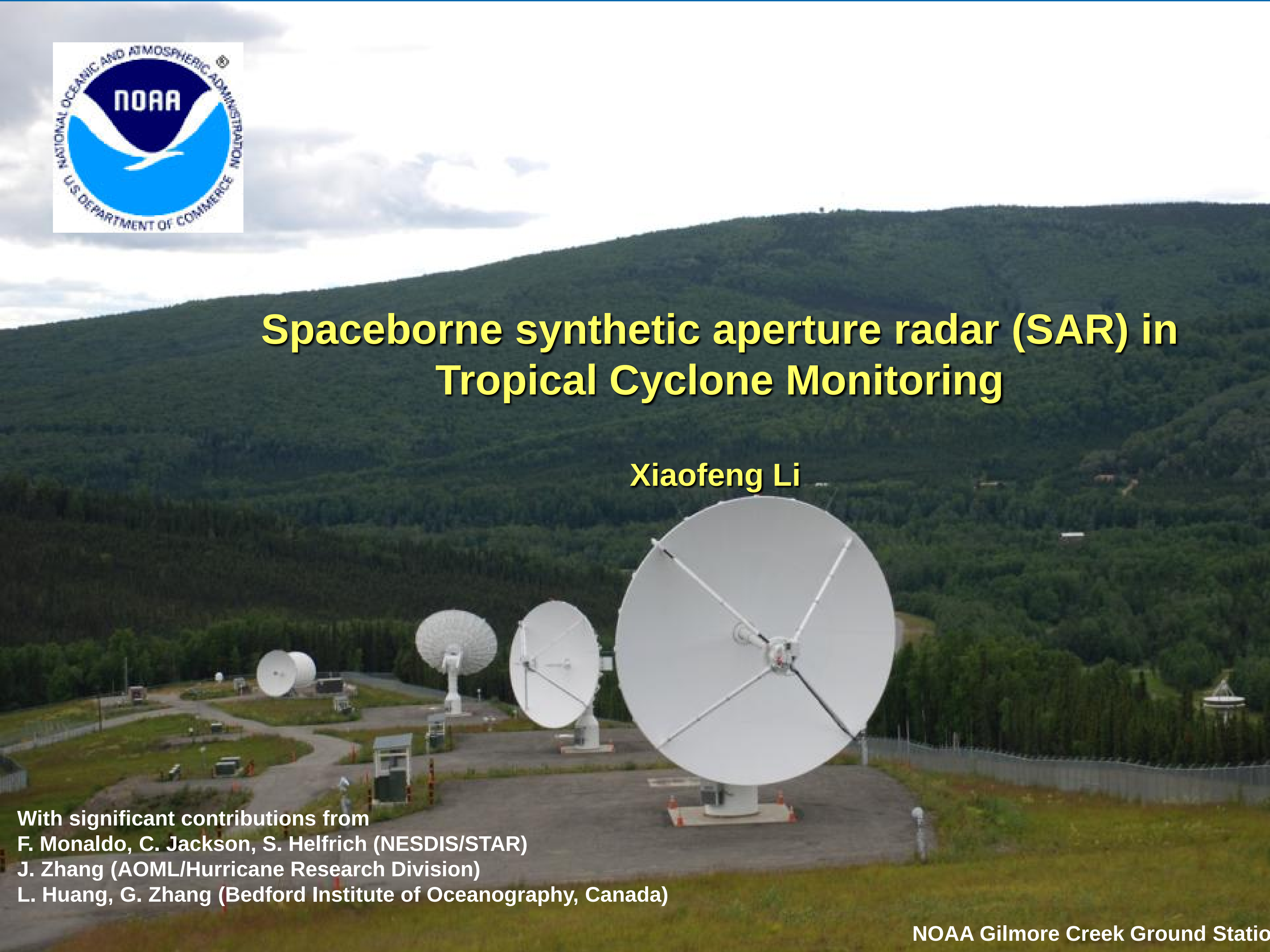

Spaceborne synthetic aperture radar (SAR) in Tropical Cyclone Monitoring

Xiaofeng Li

With significant contributions from
F. Monaldo, C. Jackson, S. Helfrich (NESDIS/STAR)
J. Zhang (AOML/Hurricane Research Division)
L. Huang, G. Zhang (Bedford Institute of Oceanography, Canada)

NOAA Gilmore Creek Ground Statio

Outline

1. Synthetic Aperture Radar (SAR) introduction

2. SAR Hurricane Morphology

3. SAR Hurricane Winds

4. SAR Hurricane Rain

5. SAR Hurricane Waves

6. Summary

1. SAR introduction - What is SAR?

Remote Sensing Oceanography – Measuring ocean from space with dedicated instruments for research and operation

Passive Remote Sensing

- **Sea surface temperature (Radiometer)**
- **Ocean Color (Radiometer)**
- **Salinity (Radiometer)**

Active Remote Sensing

- **Sea surface dynamic topography (Altimeter)**
- **Sea surface wind (Scatterometer)**
- **2-D sea surface roughness (*Synthetic Aperture Radar*)**

1. SAR introduction - What is SAR?

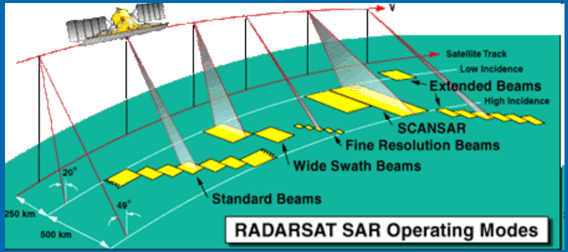

Real Aperture Radar (RAR vs SAR)

Range Resolution: Typical radar pulse bandwidths range between 10 and 40 MHz, that produce a slant range resolution , c/2β , between 15 and 3.7 meters. Range resolution is the same for RAR and SAR.

TABLE 1.3: Spatial Resolution Functional Relationships

Spatial Direction	SAR	RAR
Cross-Range (Along - Track)	$\frac{\text{Along-Track Antenna Length}}{2}$	$\frac{\text{Wavelength x Target Range}}{\text{Along-Track Antenna Length}}$
Range	$(\frac{c}{2\beta})$	$(\frac{c}{2\beta})$

1. SAR introduction - What is SAR?

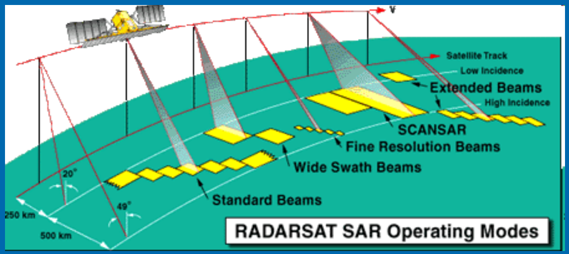

Real Aperture Radar (RAR vs SAR)

Azimuth Resolution:

RAR: $\left(\frac{\lambda}{D}R\right)$

Airborne: Airborne system in X-Band, 25 MHz bandwidth, 3 m antenna, 3000 m
Range Resolution = 6 m; Azimuth Resolution = 30 m

Spaceborne: satellite system in X-Band, 25 MHz bandwidth, 12 m antenna, 800 km
Range Resolution = 6 m; Azimuth Resolution = 2000 m not suitable for space observations

SAR: Along-Track Antenna Length/2. Realized through coherent radar signal processing. **Independent of Range and Radar Frequency and Improves with Smaller Real Antenna Aperture**

Azimuth Resolution = m -10’s m.

1. SAR introduction - What is SAR?

A Synthetic Aperture Radar (SAR) is a coherent sidelooking system which utilizes the flight path of the aircraft or spacecraft to simulate an extremely large antenna or aperture electronically and that generates high-resolution remote sensing imagery.

Synthetic Aperture Radar (SAR) instruments are active microwave instruments operating at cm wavelengths (X-band: 3 cm, C-band: 5 cm, L-band: 23 cm).

High resolution (1 m – 150 m) is achieved by signal processing of the backscattered radar signal (both amplitude and phase).

Single beam swath widths are 30-150 km. Time multiplexed multi-beam (called ScanSAR) swath widths are typically 100-500 km.

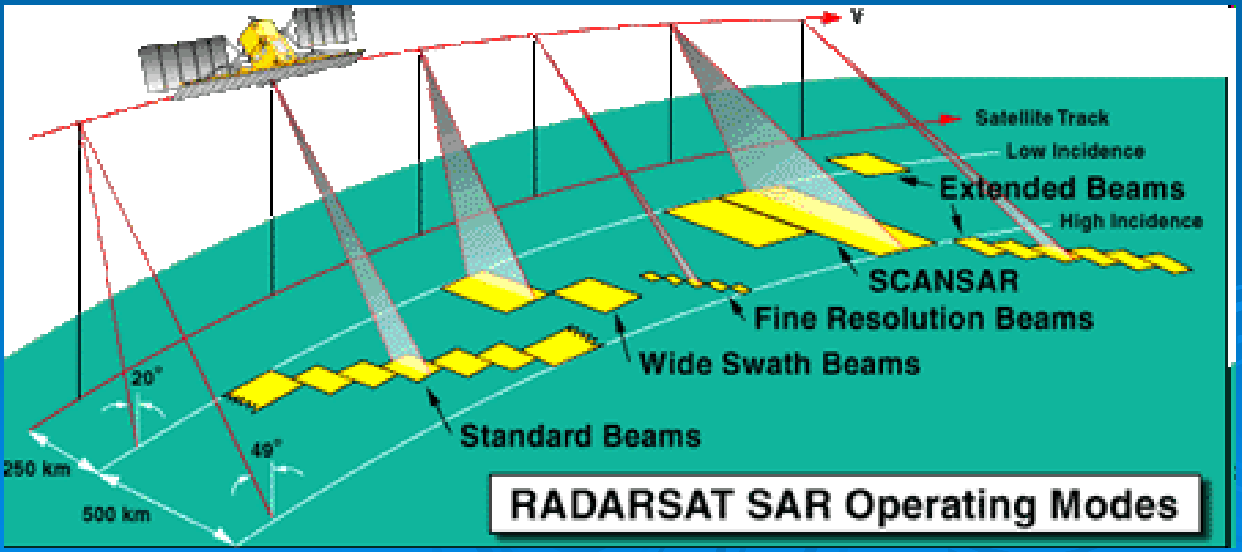

What is New About SAR Technology?

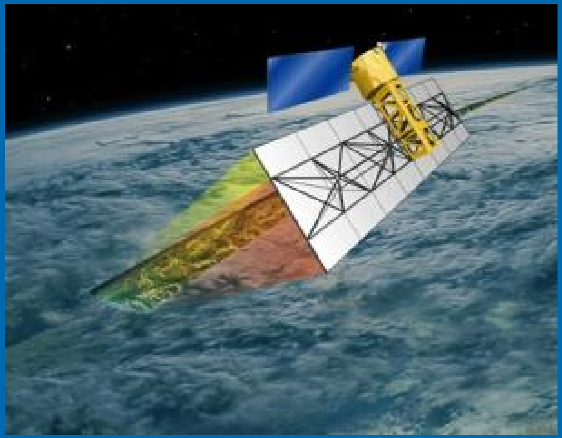

SAR is not so much a new technology :

Carl Atwood Wiley was an American mathematician and Engineer, known as the inventor of synthetic aperture radar (Patent in 1954) .

First spaceborne SAR was one of the 4 payloads on the first ocean-targetted Satellite, Seasat, launched in 1978.

This technology is maturing to the point of becoming operational

Land applications: generating DEM, earthquake surface change, soil moisture, forestry, land/vegetation classification, etc.

Ocean and atmospheric applications: sea ice, wind, wave, current, glacier etc.

Recent developments include:

- **Data available from many satellites (more than 10 currently operating)**
- **Multiple Frequencies – X, C, L**
- **Multiple polarizations – Dual and quad polarization**
- **Interferometry - Along-track and cross-track in addition to repeat pass**
- **Operational satellite constellations under development in Europe and Canada**
- **Maybe, finally, another U.S. SAR – DESDynI (and SMAP)**

Synthetic Aperture Radar (SAR) Data Sources

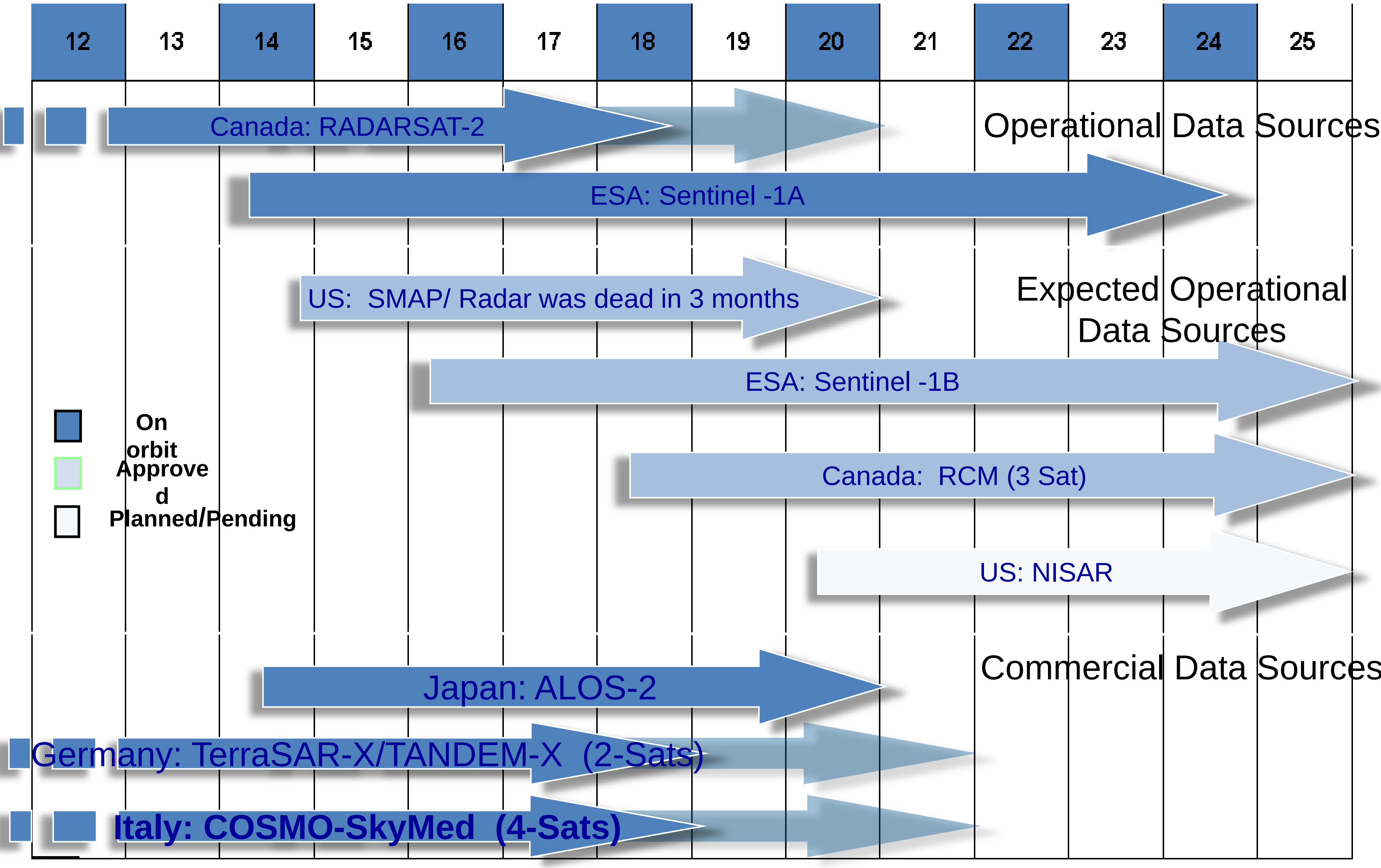

1. SAR introduction - continued

SAR Advantageous Characteristics for Environmental Applications

- Active sensor VS Passive sensor
- Microwave VS IR/Visible
- Small coverage (450 km) VS Large coverage (1000 km swatch)
- All weather VS Cloud free
- Day/night VS Day (visible), Day/Night IR
- High Spatial Resolution VS Low resolution (250m, 1 km)
- Adjacent land does not contaminate ocean observations (right up to the coast and in bays/straits)
- Phase preserving processing allows interferometric applications able to sense mm changes in topography

1. SAR introduction - continued

Main Demonstration Products

1. High Resolution Ocean and Coastal SAR Imagery
2. Ocean Surface Wind Maps and Vectors
3. Hard Target (ship) Locations
4. Oil Spills
5. Swell Waves

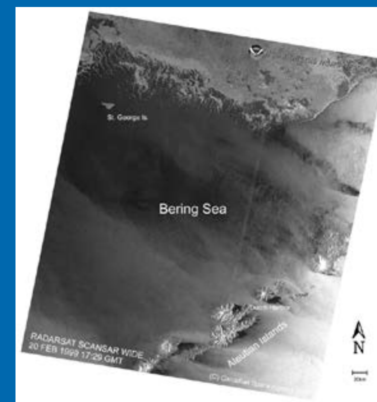

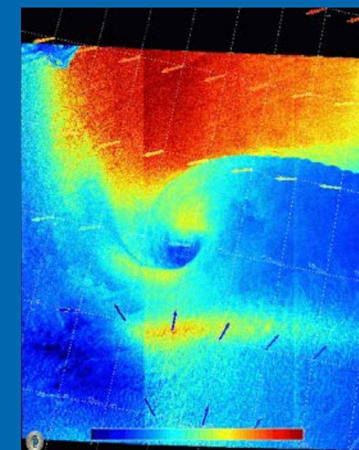

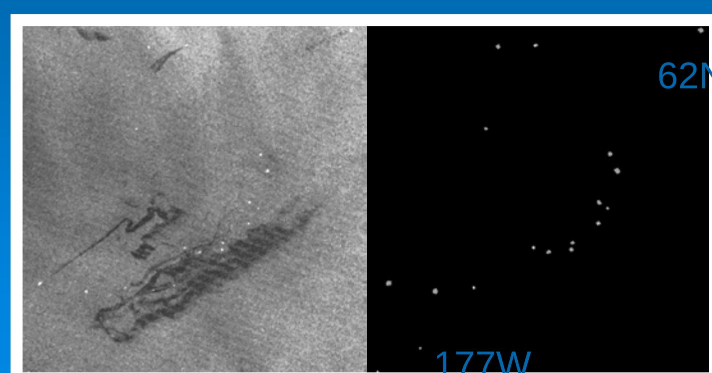

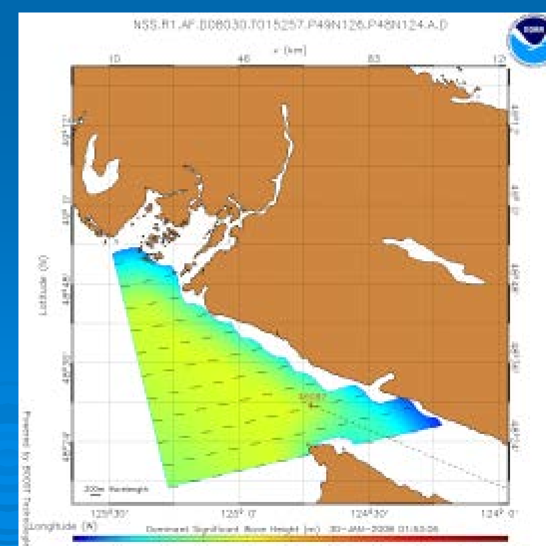

1. SAR introduction –
A Suite of Products from SAR Cyclone Imagery

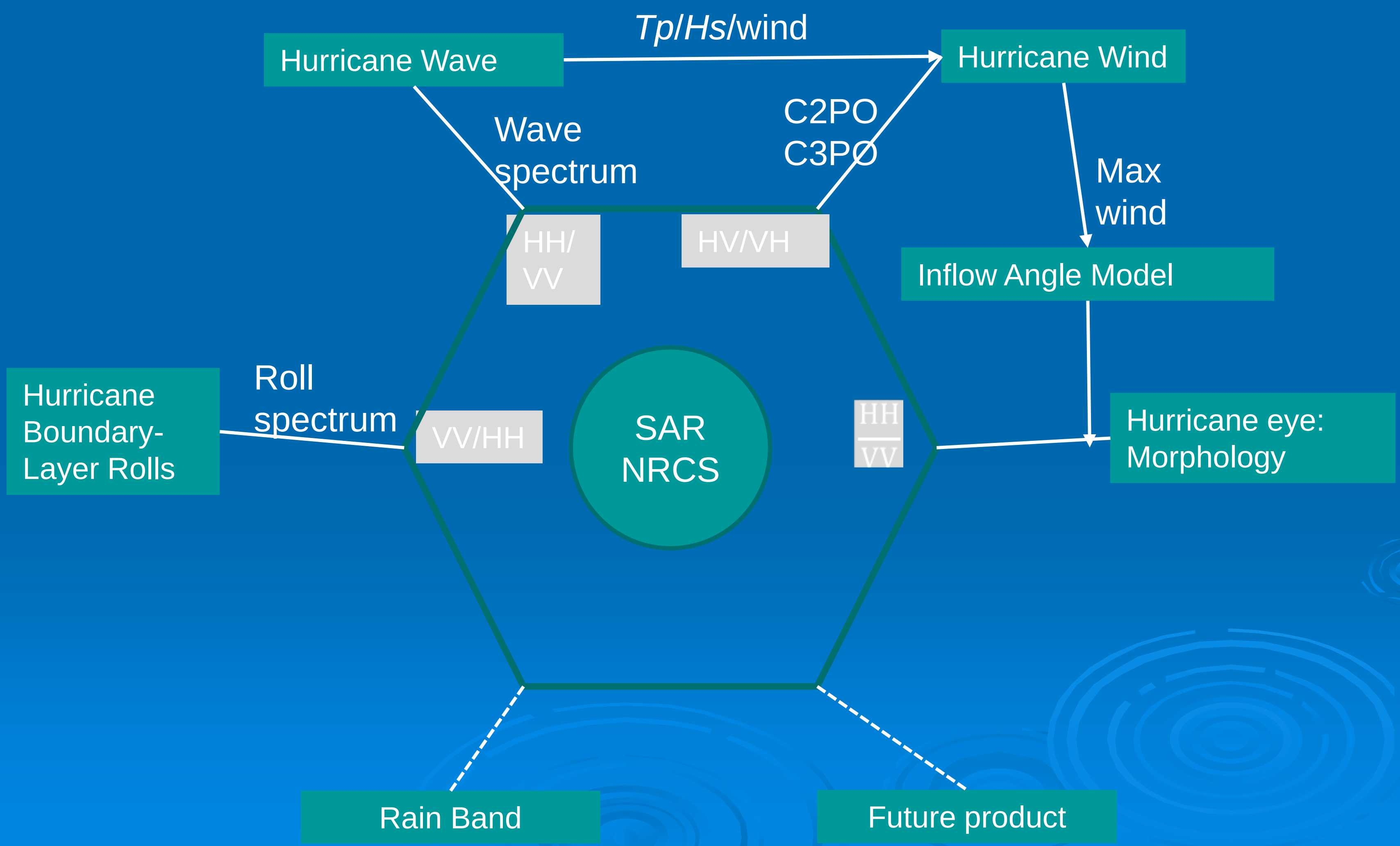

2 Tropical cyclone morphology from SAR

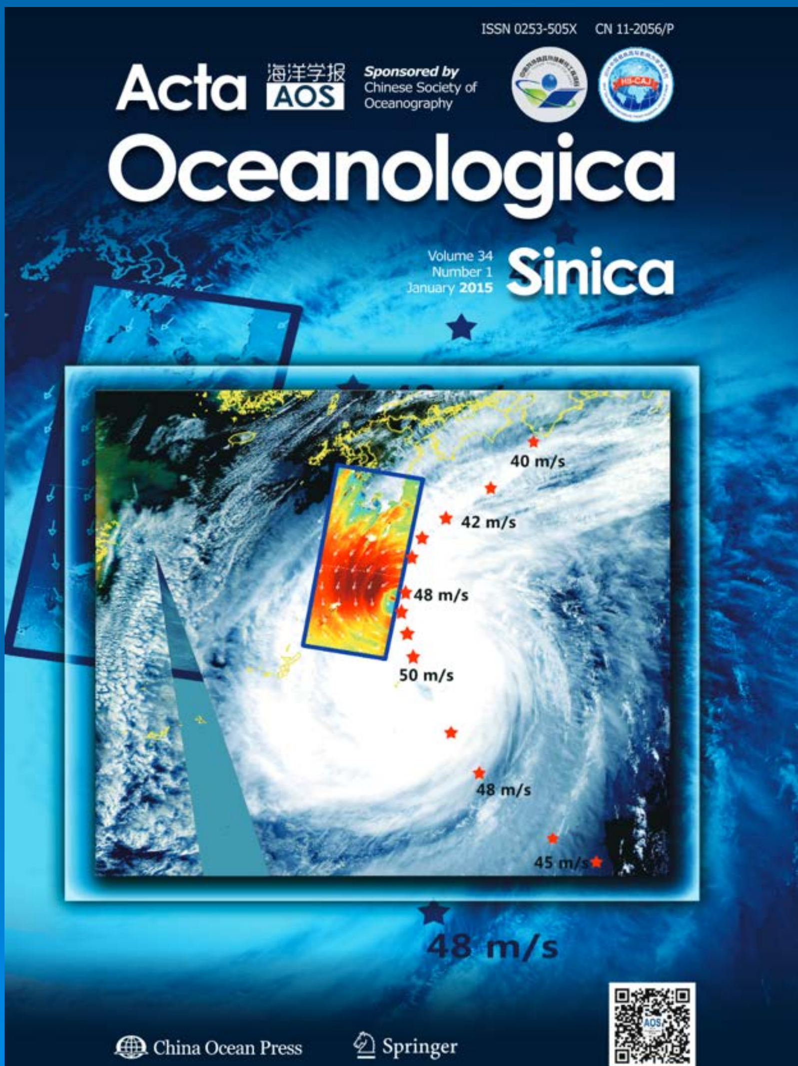

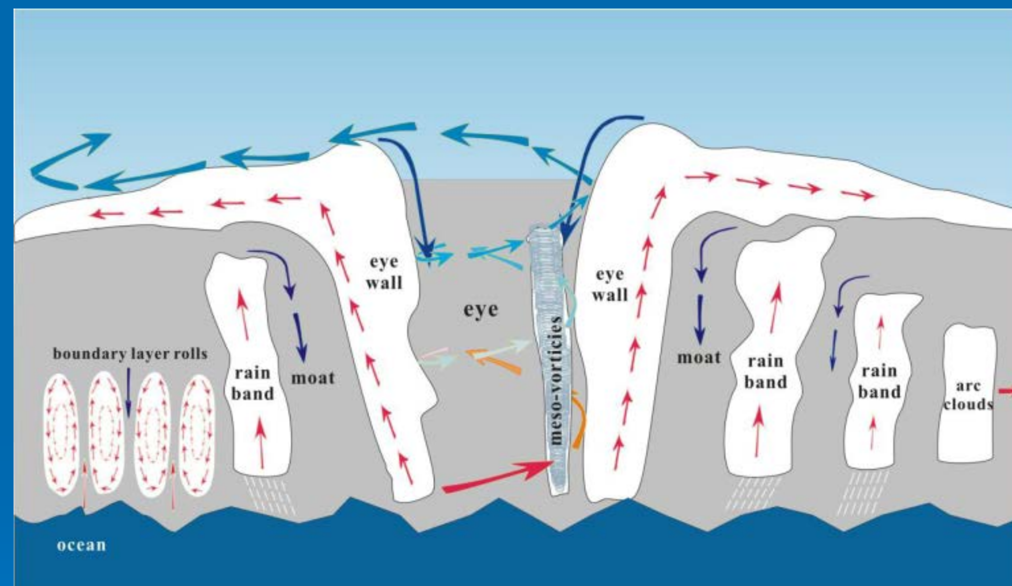

Schematic plot of tropical cyclone structure and atmospheric phenomena including eye/eyewall, rain band, boundary layer rolls, arc cloud, and meso-vorticies (not to scale).

2 Tropical cyclone morphology from SAR
- different eye shape

- Hurricane center
- Eye shapes: Circular, Ellipse, Triangular, Rectangular
- Rain cells detection

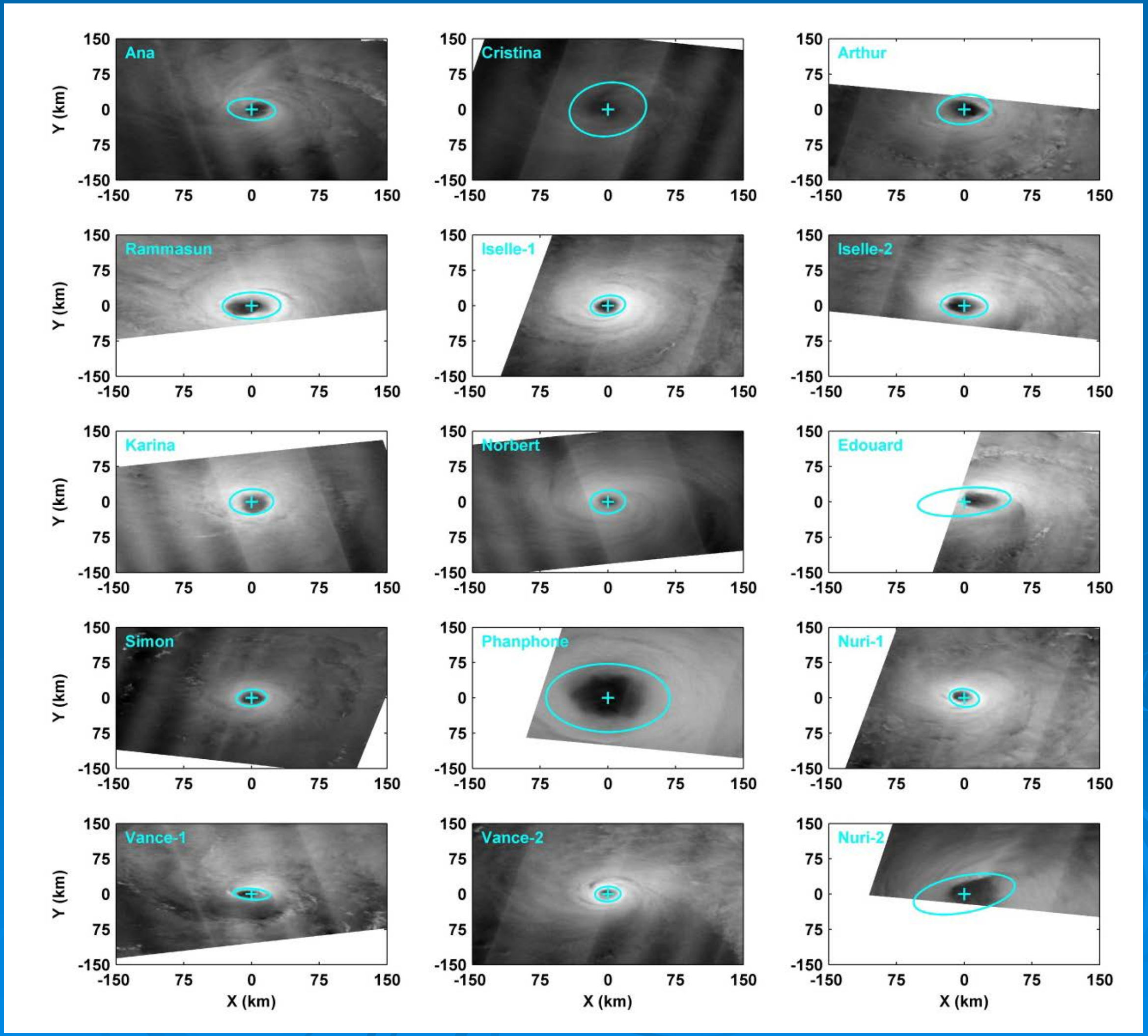

2 Tropical cyclone morphology from SAR
- different eye-wall shape

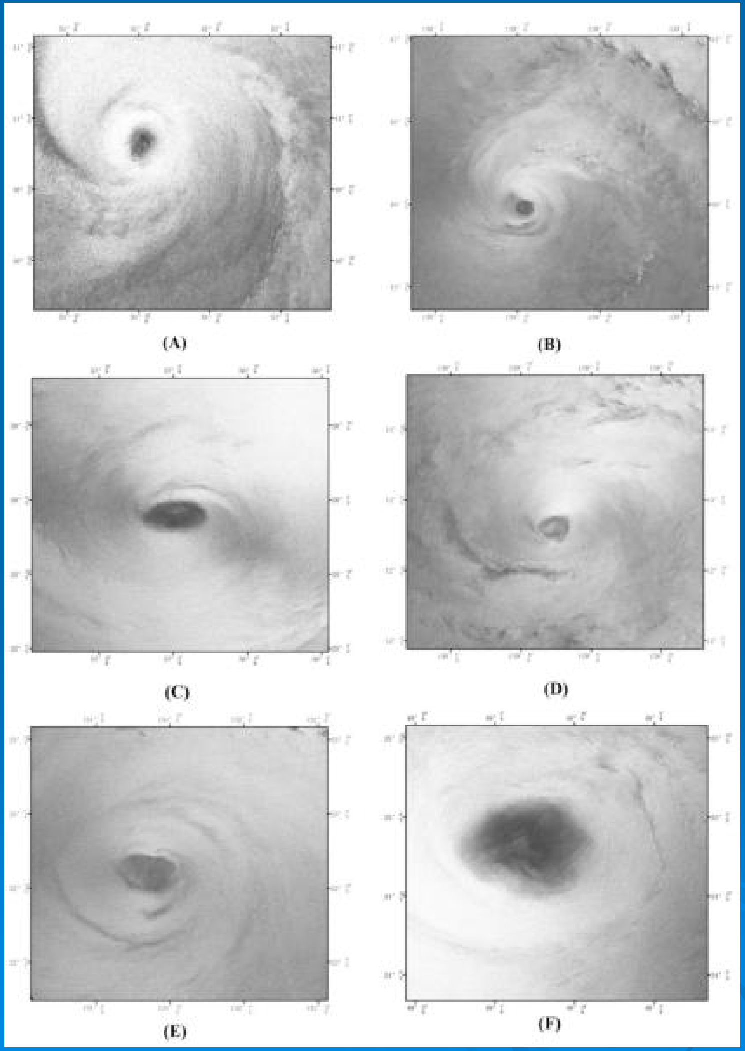

73 RADARSAT-1 images
10 ENVISAT images

Wavenumber 0. circular shape with concentric eyewall
Wavenumber 1. circular eye with asymmetric eyewall
Wavenumber 2. elliptical-shaped eye
Wavenumber 3. triangular-shaped eye
Wavenumber 4. square- or rectangular-shaped eye
Wavenumber 5. pentagon eye

Examples of SAR hurricanes with different eye wall types.
(A) Wavenumber 0. Hurricane IVAN, 2004-9-6 09:06:22
(B) Wavenumber 1. Hurricane KENNETH, 2005-9-25 03:21:45
(C) Wavenumber 2. Hurricane HELENE, 2006-9-20 21:52:31
(D) Wavenumber 3. Hurricane JOVA, 2005-9-18 03:25:08
(E) Wavenumber 4. Typhoon GUCHOL, 2005-8-22 20:38:52
(F) Wavenumber 5. Hurricane ERIN, 2001-9-13 10:03:10

2 Tropical cyclone morphology from SAR
- Wavenumber asymmetry and hurricane eye size versus maximum hurricane wind

The number of SAR observations showing different tropical cyclone eye shapes

wavenumber	0	1	2	3	4	5
number of SAR images	5	20	20	5	9	2
Max eye area (km^2)	382	2984	3138	1632	6047	5610
Mean eye area (km^2)	176	743	1604	857	2945	4531
Min eye area (km^2)	32	90	366	212	956	3452

73 RADARSAT-1 images
10 ENVISAT images

Wavenumber 0. circular shape with concentric eyewall
Wavenumber 1. circular eye with asymmetric eyewall
Wavenumber 2. elliptical-shaped eye
Wavenumber 3. triangular-shaped eye
Wavenumber 4. square- or rectangular-shaped eye
Wavenumber 5. pentagon eye

- Majority of data exhibit wavenumber 1 and 2 asymmetries in the eye, suggesting that the nature of the inner core asymmetry is dominated by these two wavenumbers.

- The size of the eye ranges from hundreds to thousands of square kilometers.

2 Tropical cyclone morphology from SAR
- Eye and Rain Band Extraction

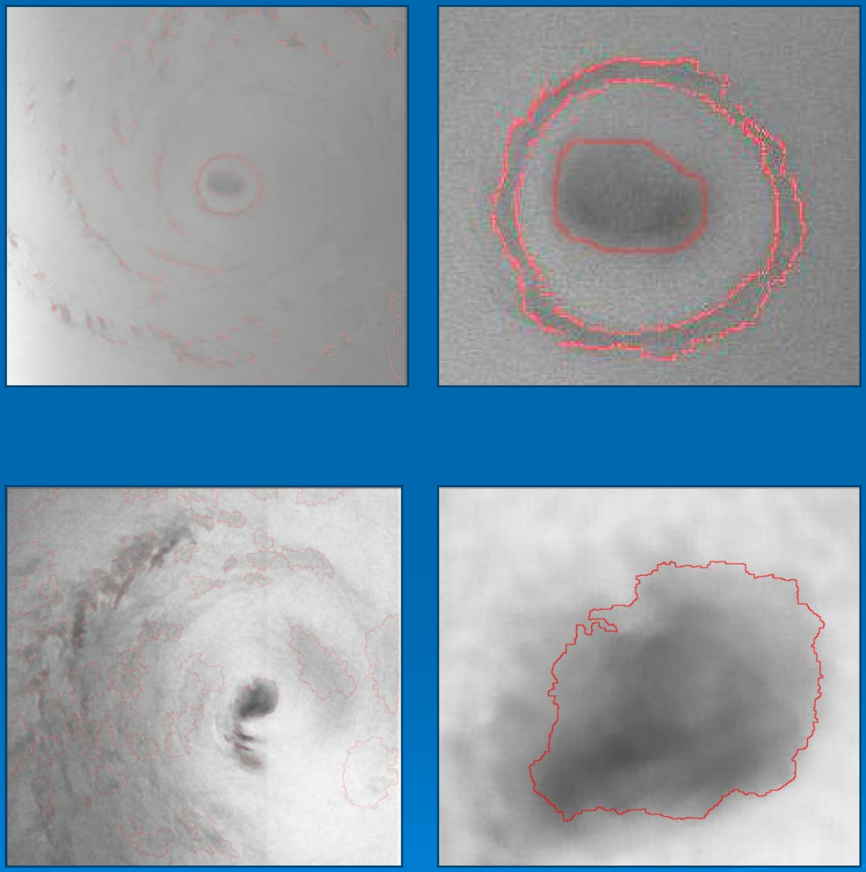

Hurricane eye
(Hurricane Katrina, 2005)

SAR image segmentation

- ➢top-hat transfer to reduce the noise
- ➢Labeled watershed transform to extract the hurricane eye

S. Jin *et al*, *IEEE GRSL 2016*

2 Tropical cyclone morphology from SAR
- Fine structure

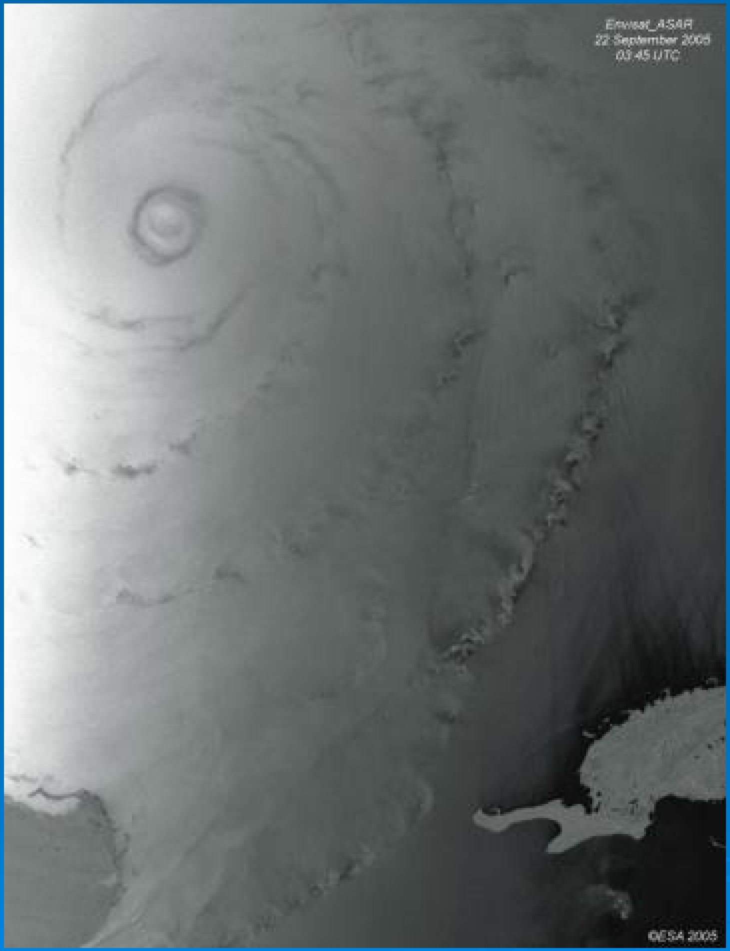

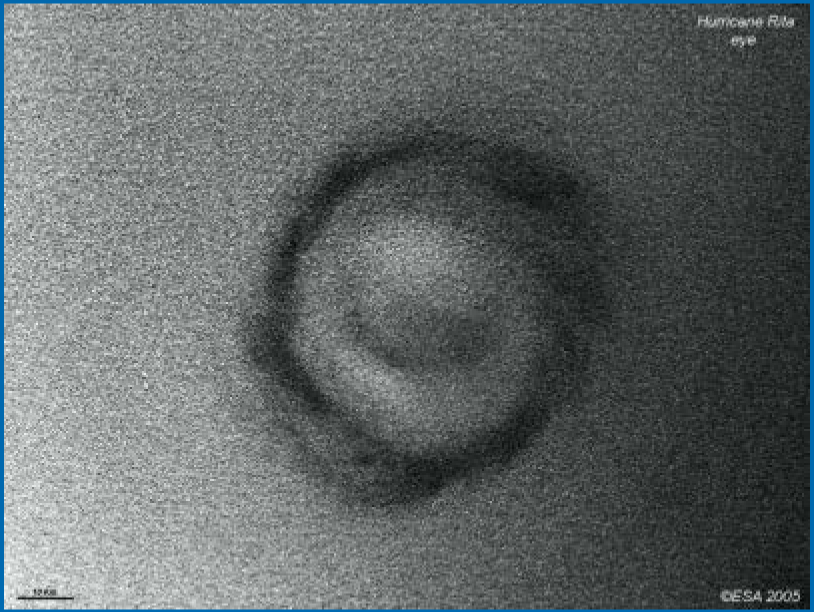

- Very fine and detailed structure;
- High backscatter within the eye;
- Wave patterns around the eye wall;
- A series of convective cells.

2 Tropical cyclone morphology from SAR
- Boundary layer rolls

Dataset

Information of SAR Images of the Six TC's

Tropical cyclones	Date/time (UTC)	Satellite	Polarization	Swath (km)	Image number	Storm center (lat,lon)	Hemisphere for location of storm center	Category
Earl	2 Sep 2010 22:59	RADARSAT-2	VV/VH	500	1	(32.779°, −74.802°)	North	Hurricane 3
Fanapi	17 Sep 2010 21:14	RADARSAT-2	HH/HV	500	1	(23.434°, 126.597°)	North	Hurricane 2
Malakas	22 Sep 2010 20:31	RADARSAT-2	HH/HV	500	1	(19.566°, 141.436°)	North	Severe tropical storm
Megi	15 Oct 2010 21:00	RADARSAT-2	VV	500	1	(16.985°, 133.575°)	North	Hurricane 1
Katrina	28 Aug 2005 15:51	ENVISAT	VV	400	1	(26.187°, −88.215°)	North	Hurricane 5
Katrina	28 Aug 2005 23:50	RADARSAT-1	VV	500	1	(27.162°, −89.228°)	North	Hurricane 5
Irma	7 Sep 2017 10:30	SENTINEL-1A	VV/VH	250	3	(20.050°, −68.650°)	North	Hurricane 5
Jose	8 Sep 2017 22:03	SENTINEL-1A	VV/VH	250	4	(16.635°, −58.475°)	North	Hurricane 4
Maria	21 Sep 2017 22:45	SENTINEL-1A	VV/VH	250	3	(20.858°, −69.917°)	North	Hurricane 3

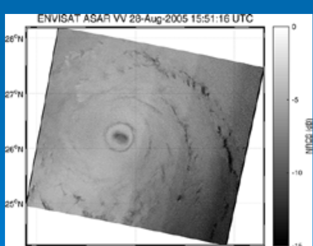

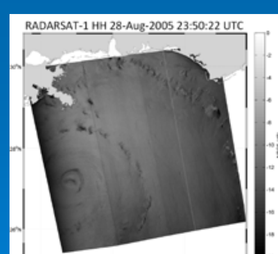

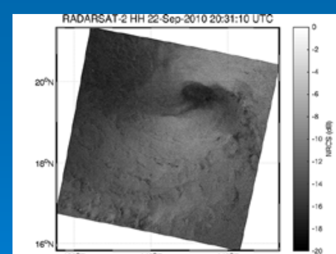

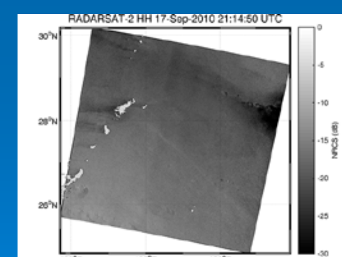

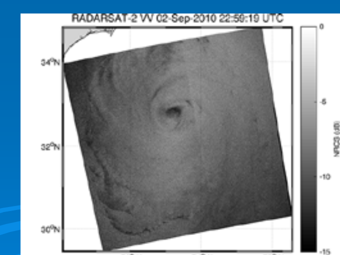

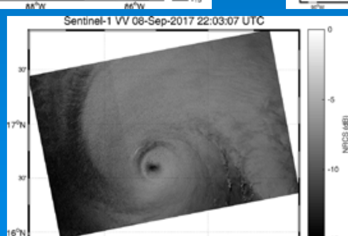

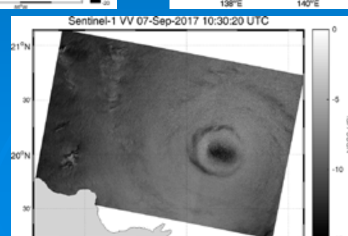

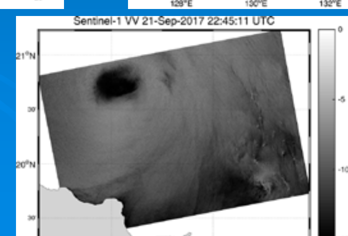

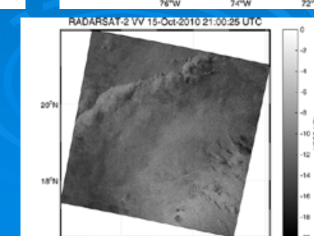

2 Tropical cyclone morphology from SAR - Boundary layer rolls

Methodology: Extraction of Roll Characteristics

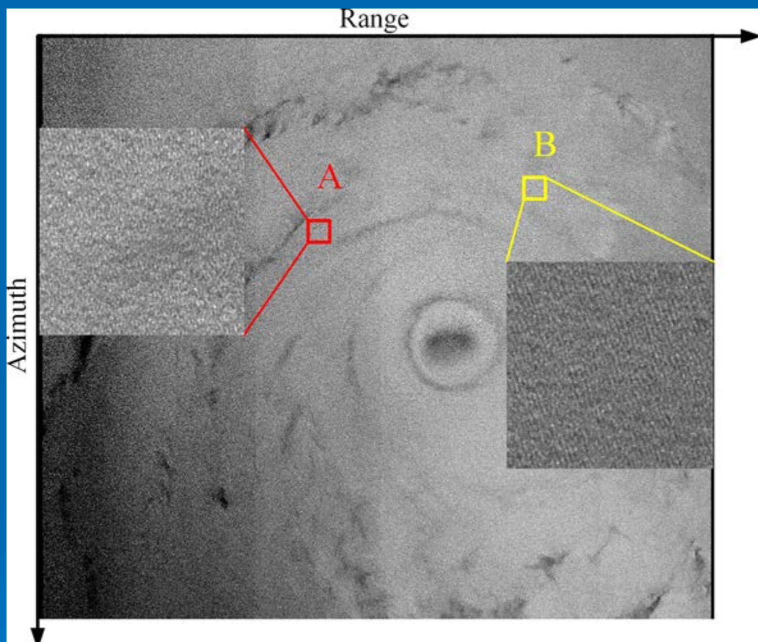

Hurricane Katrina 2005 acquired by ENVISAT

2D-FFT

A

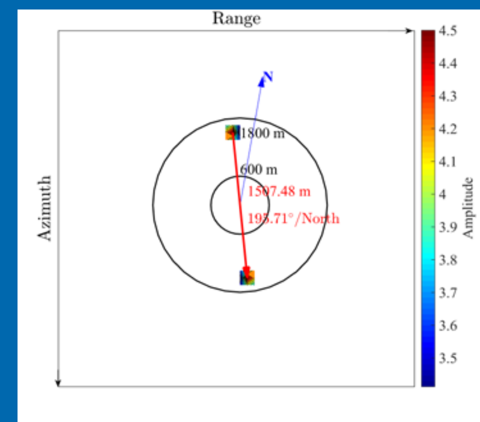

B

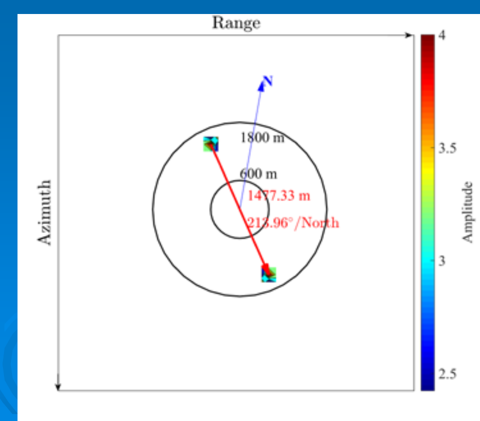

Two dimensional FFT analysis of SAR image shows the dominant wavelength and orientation of the boundary layer rolls with 180 degree ambiguity.

2 Tropical cyclone morphology from SAR
- Boundary layer rolls

Results: Occurrence of Rolls

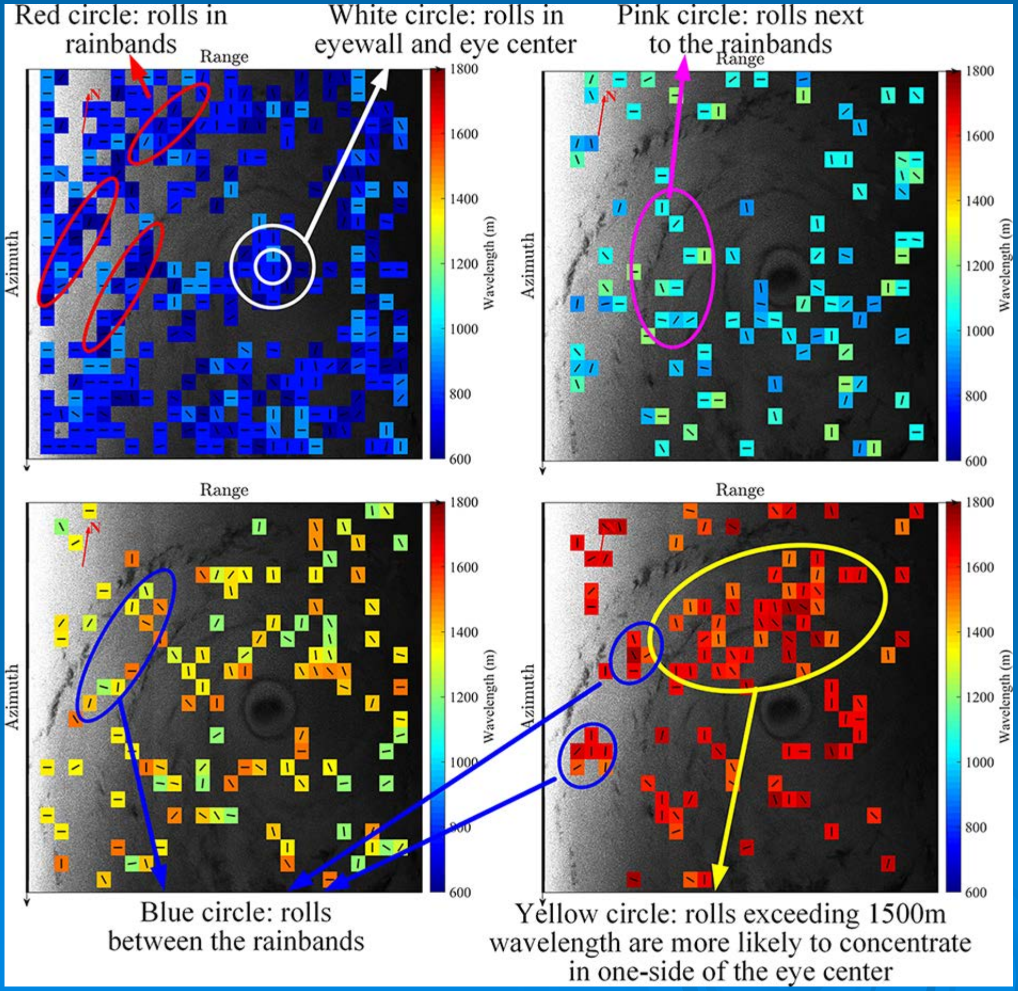

Hurricane Katrina 2005 acquired by ENVISAT

- The roll wavelengths < 900 m: mostly locate at the eye center, eyewall, rainbands, or at distances larger than 200 km to hurricane center;
- The roll wavelengths 900 -1200 m: locate next to rainbands or next to the eyewall;
- The roll wavelengths 1200 -1500 m: locate out of the eyewall or between the rainbands;
- The roll wavelengths >1500 m: concentrate in the location near to the out side regions of eyewall.

- the spatial distribution of roll wavelengths is asymmetrical: the rolls with wavelength exceeding 1500 m are more likely to concentrate in one side relative to storm center. This may due to the asymmetric convection and wind profiles within the TC's.

2 Tropical cyclone morphology from SAR
- Boundary layer rolls

Results: Roll Wavelengths Distribution with Respect to Storm Center

Roll Wavelengths at Different Locations Relative to the Storm Centers

Name of TC\wave-length (m)\ distance (km)	0–15	15–30	30–40	40–70	70–100	100–145	145–175	175–200	>200
Earl	800	1,111	1,268	1,193	**1,340**	1,278	1,167	1,152	1,126
Fanapi									998
Malakas	705	787	732	909	991	1,026	**1,040**	919	920
Megi	767	1,042	1,042	**1,135**	1,097	984	972	993	922
Katrina-ENVISAT	750	773	890	1,248	**1,278**	1,038	968	1,052	972
Katrina-RADARSAT-1	1,270	1,236	1,028	1,238	**1,350**	1,216	1,114	1,072	1,013
Irma	909	1,003	**1,060**	947	857	899	864	843	926
Jose	1,207	1,202	**1,300**	1,263	1,250	1,256	1,250	1,182	1,195
Maria	1,050	1,089	1,155	1,241	1,260	1,388	**1,399**	1,269	1.017

The roll wavelengths at different locations relative to the storm center (*d*) are calculated.

In generally, the roll wavelengths are relatively shorter around the hurricane center. With the increasing of *d*, the roll wavelengths become longer and reach the peak values at 30-175 km distance to TC centers. After reaching the peak values, the roll wavelengths decrease with *d*.

2 Tropical cyclone morphology from SAR
- Boundary layer rolls

Results: Roll Wavelengths Distribution with Respect to Storm Center

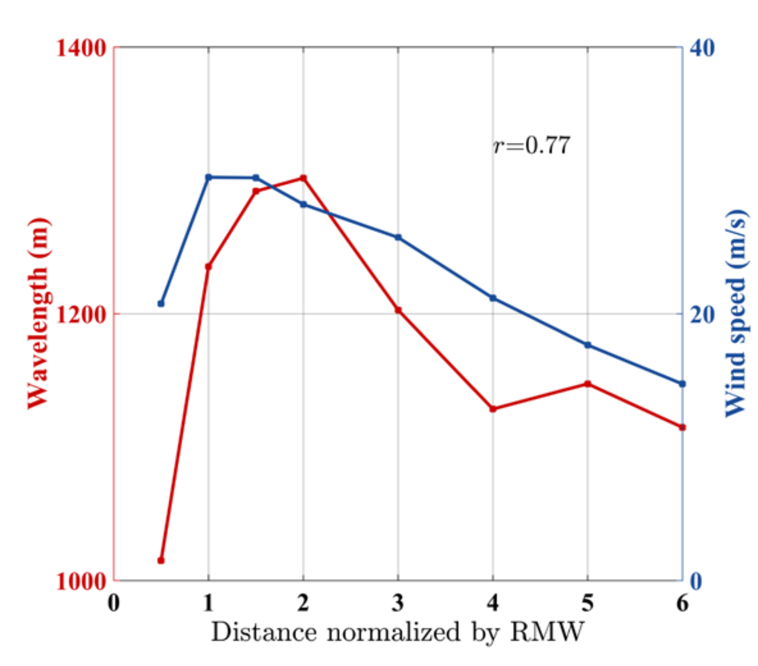

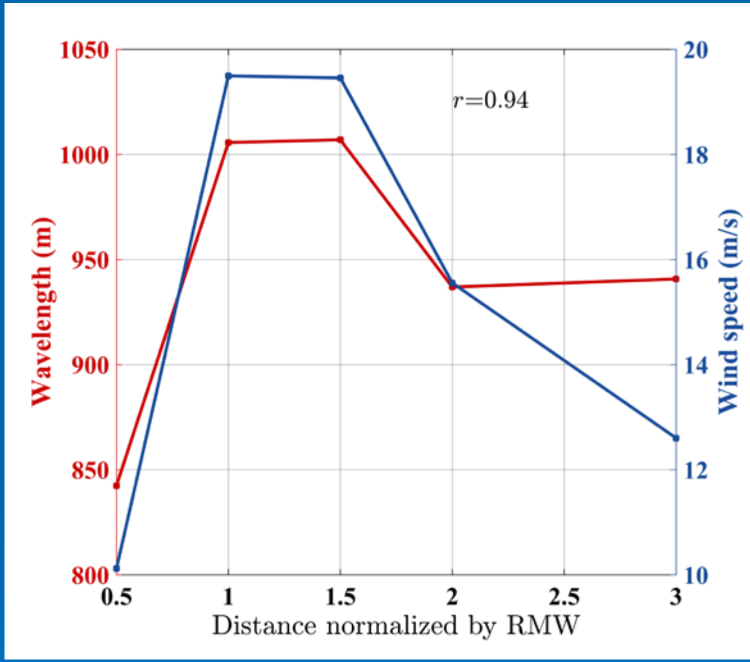

Figure: The wavelengths of rolls as a function of distance normalized by RMW. Left: Hurricane Earl; Right: Typhoon Malakas.

- The change of roll wavelength is slightly hysteretic compared to local wind speed.
- The roll wavelengths (red line) and the local wind speeds (blue line) present generally similar tendencies. The calculated correlation coefficients between them are illustrated. This demonstrates that roll characteristics are associated with the local wind speeds.
- Define d* as the distance normalized by RMW (radius of maximum wind). The wind speeds consistently decrease with d*, whereas the roll wavelengths overall decrease with d* but slightly fluctuate at larger d*.

2 Tropical cyclone morphology from SAR
- Meso-votices

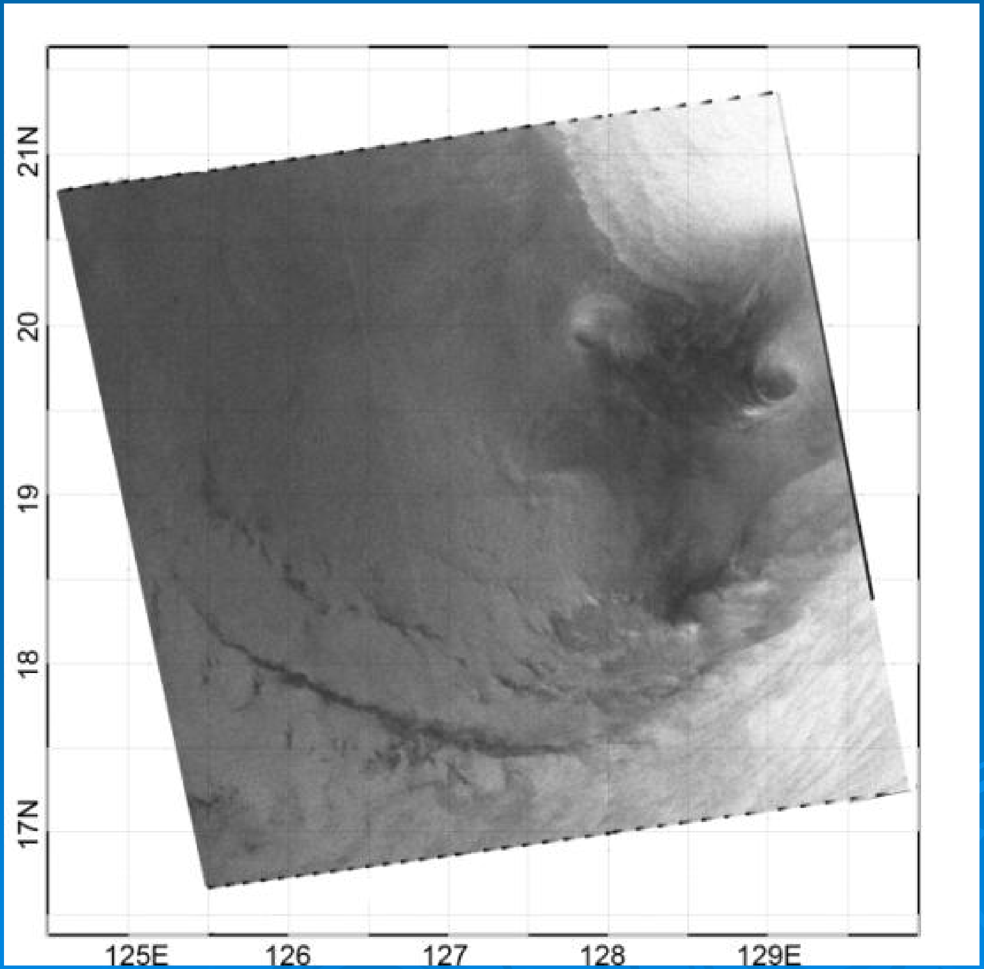

2 Tropical cyclone morphology from SAR - land-sea patterns

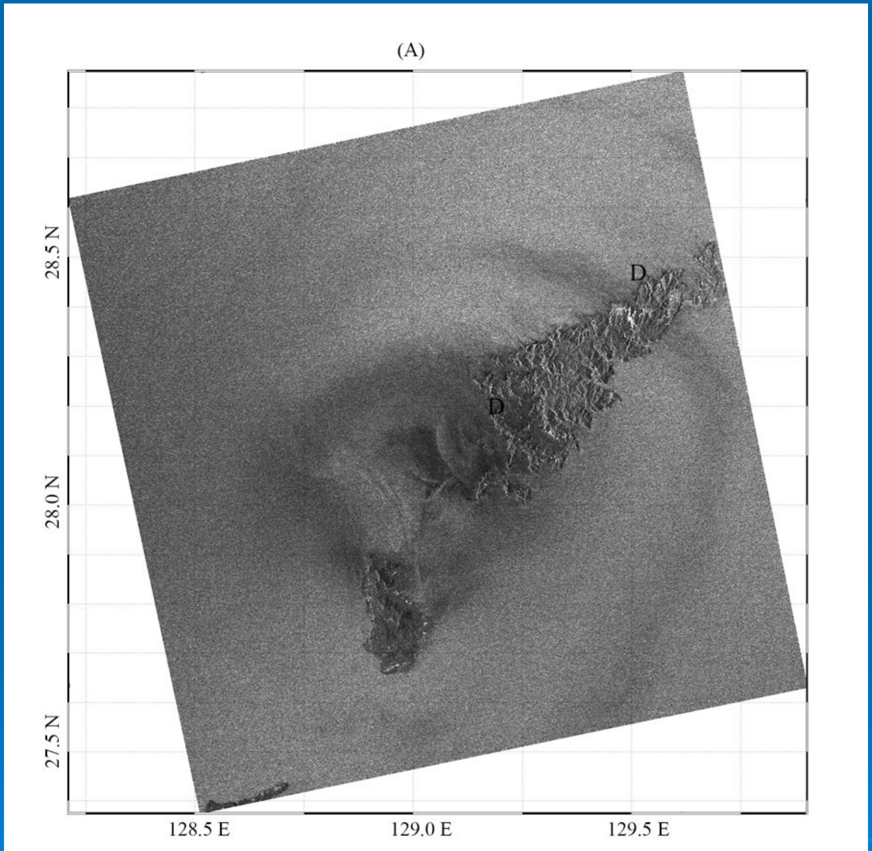

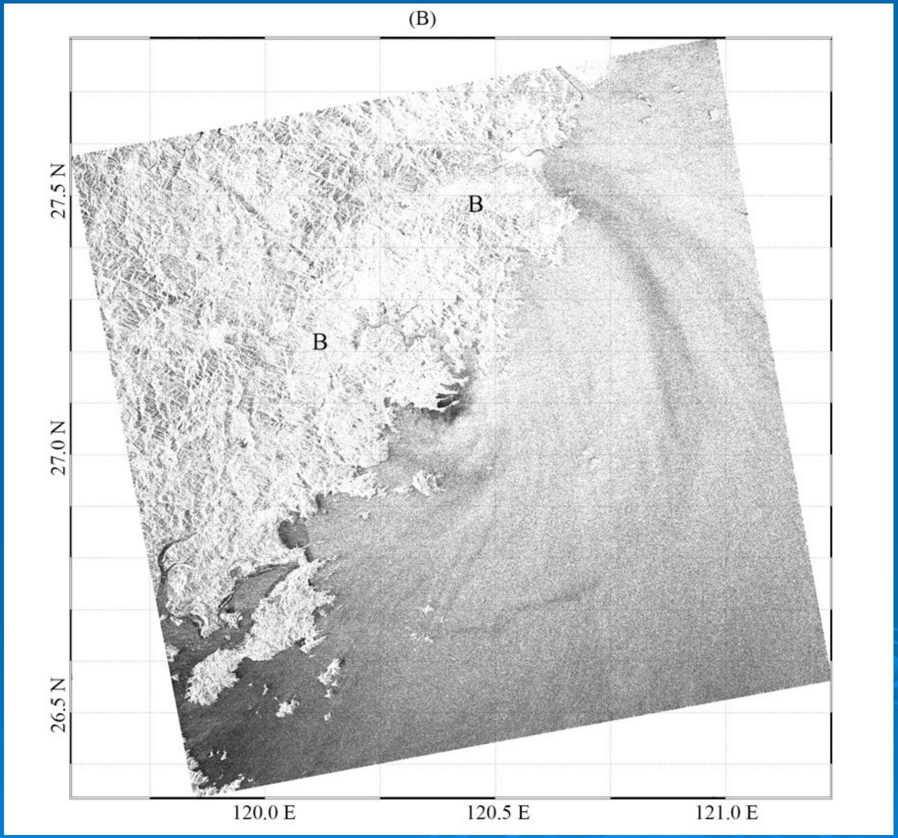

3. SAR Hurricane Winds

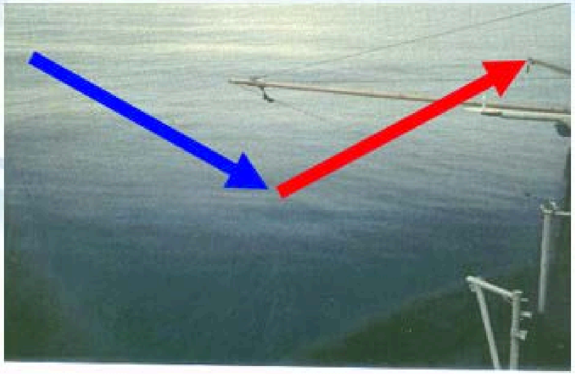

BEAUFORT FORCE 0
WIND SPEED: LESS THAN 1 KNOT

SEA: SEA LIKE A MIRROR

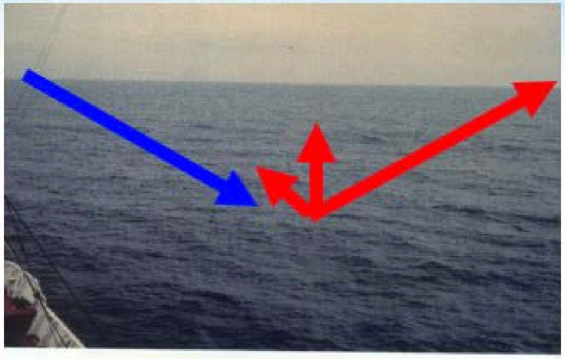

BEAUFORT FORCE 3
WIND SPEED: 7-10 KNOTS

SEA: WAVE HEIGHT .6-1M (2-3FT), LARGE WAVELETS, CRESTS BEGIN TO BREAK, ANY FOAM HAS GLASSY APPEARANCE, SCATTERED WHITECAPS

BEAUFORT FORCE 6
WIND SPEED: 22-27 KNOTS

SEA: WAVE HEIGHT 3-4M (9.5-13 FT), LARGER WAVES BEGIN TO FORM, SPRAY IS PRESENT, WHITE FOAM CRESTS ARE EVERYWHERE

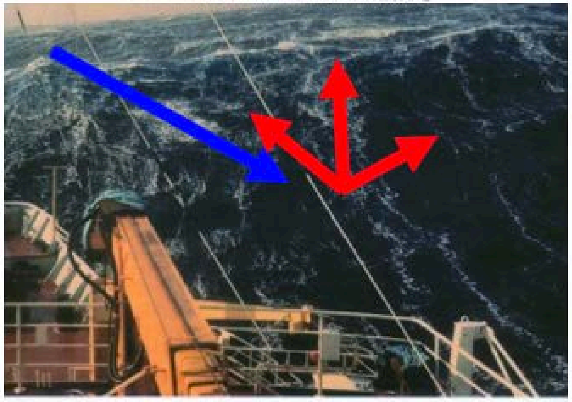

BEAUFORT FORCE 9
WIND SPEED: 41-47 KNOTS

SEA: WAVE HEIGHT 7-10M (23-32FT), HIGH WAVES, DENSE STREAKS OF FOAM ALONG DIRECTION OF THE WIND, WAVE CRESTS BEGIN TO TOPPLE, TUMBLE, AND ROLL OVER. SPRAY MAY AFFECT VISIBILITY.

1

i.ca

® Z.

3. SAR Hurricane Winds

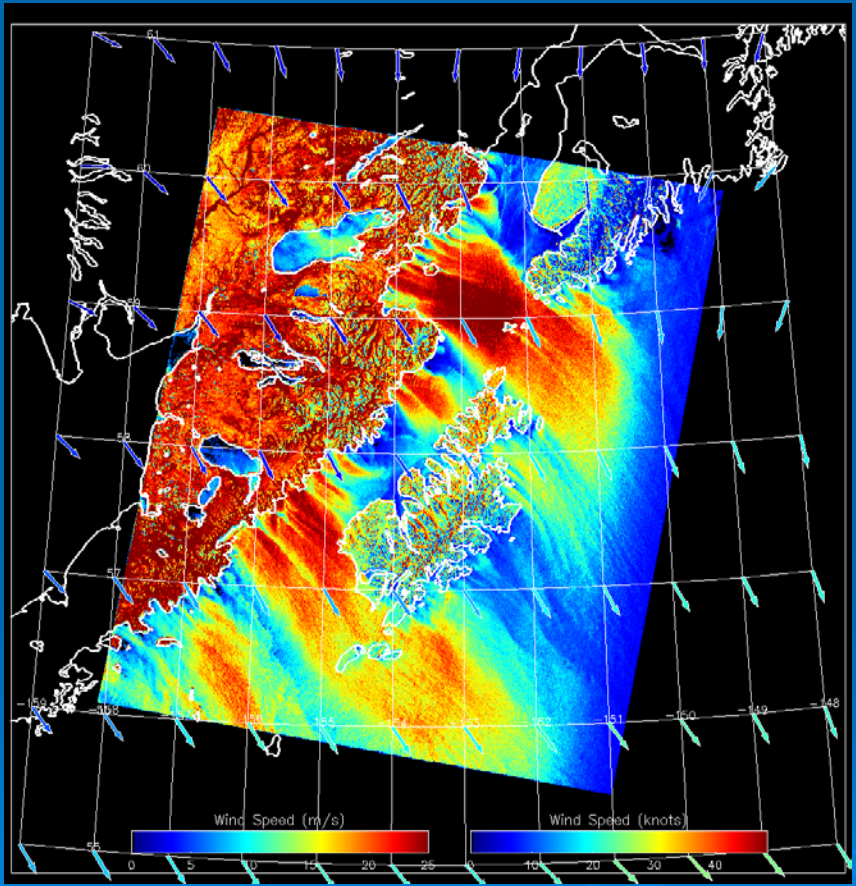

NOGAPS WIND

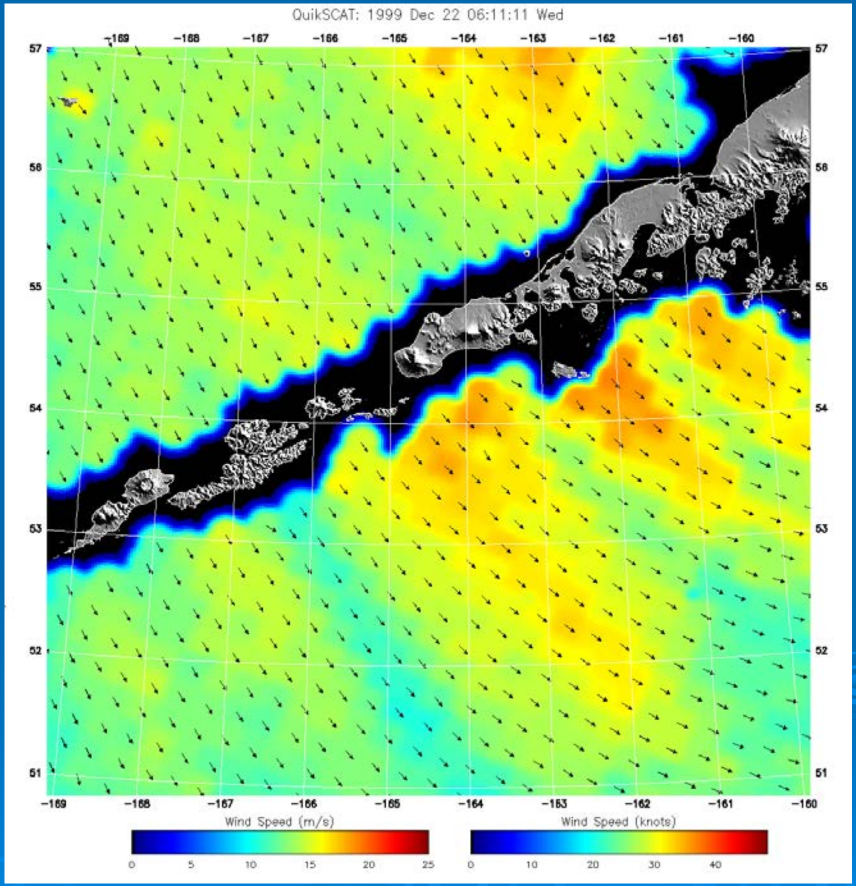

QuickScat WIND

3. SAR Hurricane Winds - GMF

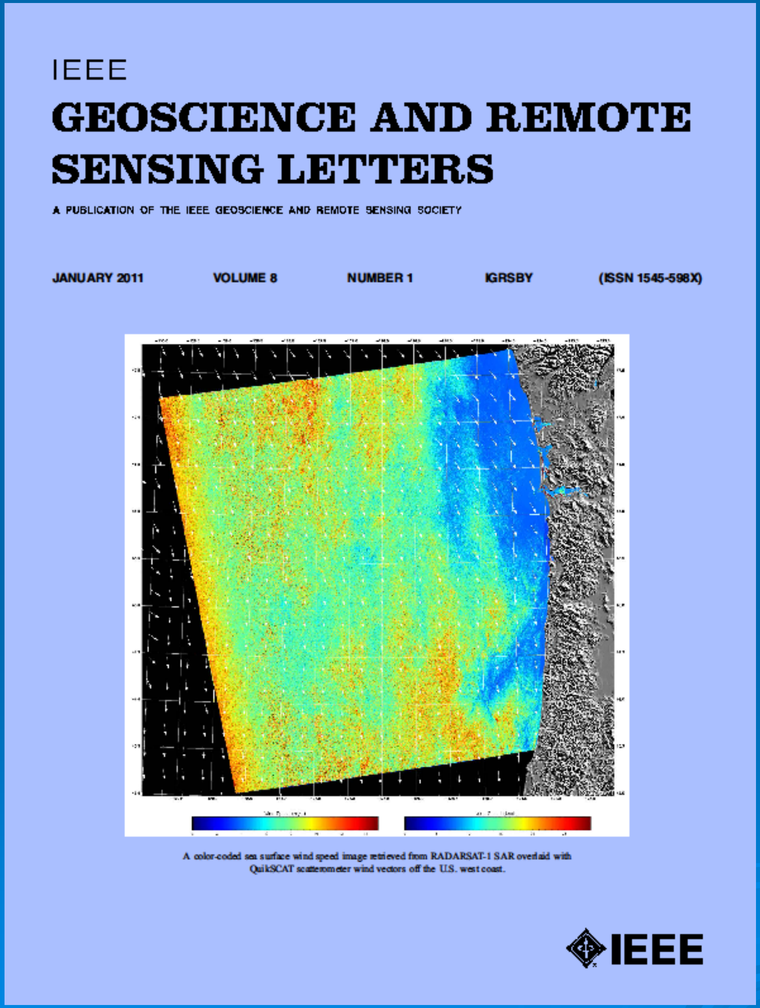

IEEE

GEOSCIENCE AND REMOTE SENSING LETTERS

A PUBLICATION OF THE IEEE GEOSCIENCE AND REMOTE SENSING SOCIETY

JANUARY 2011 VOLUME 8 NUMBER 1 IGRSBY (ISSN 1545-598X)

A color-coded sea surface wind speed image retrieved from RADARSAT-1 SAR overlaid with QuikSCAT scatterometer wind vectors off the U.S. west coast.

IEEE

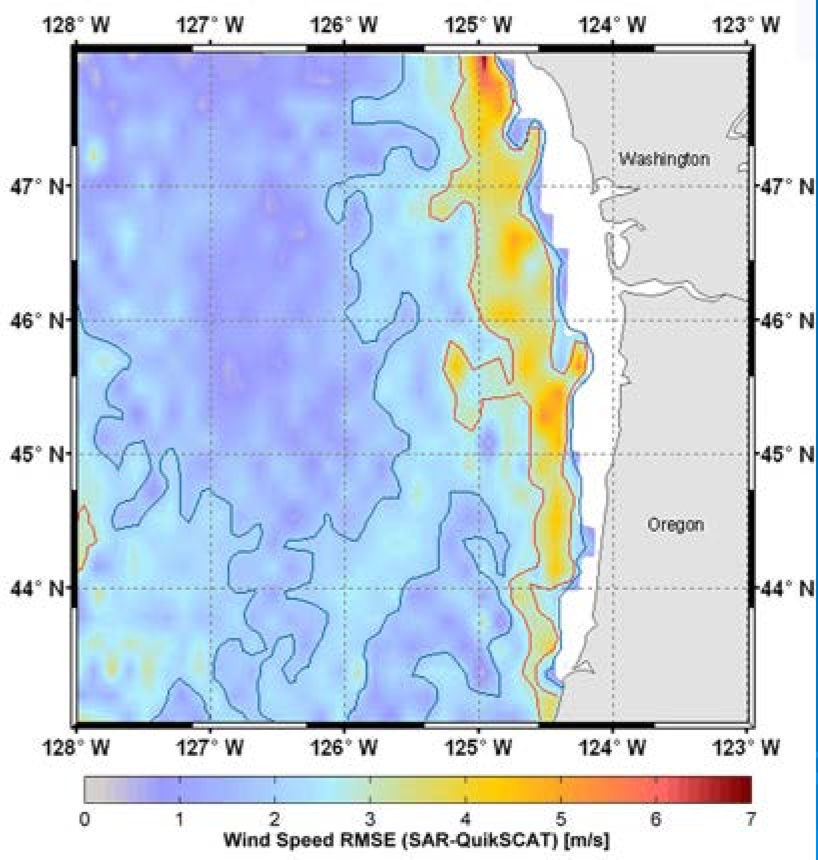

IEEE Geoscience and Remote Sensing Letters, 99, 163-167, doi: 10.1109/LGRS.2010.2053345, 2010

3. SAR Hurricane Winds

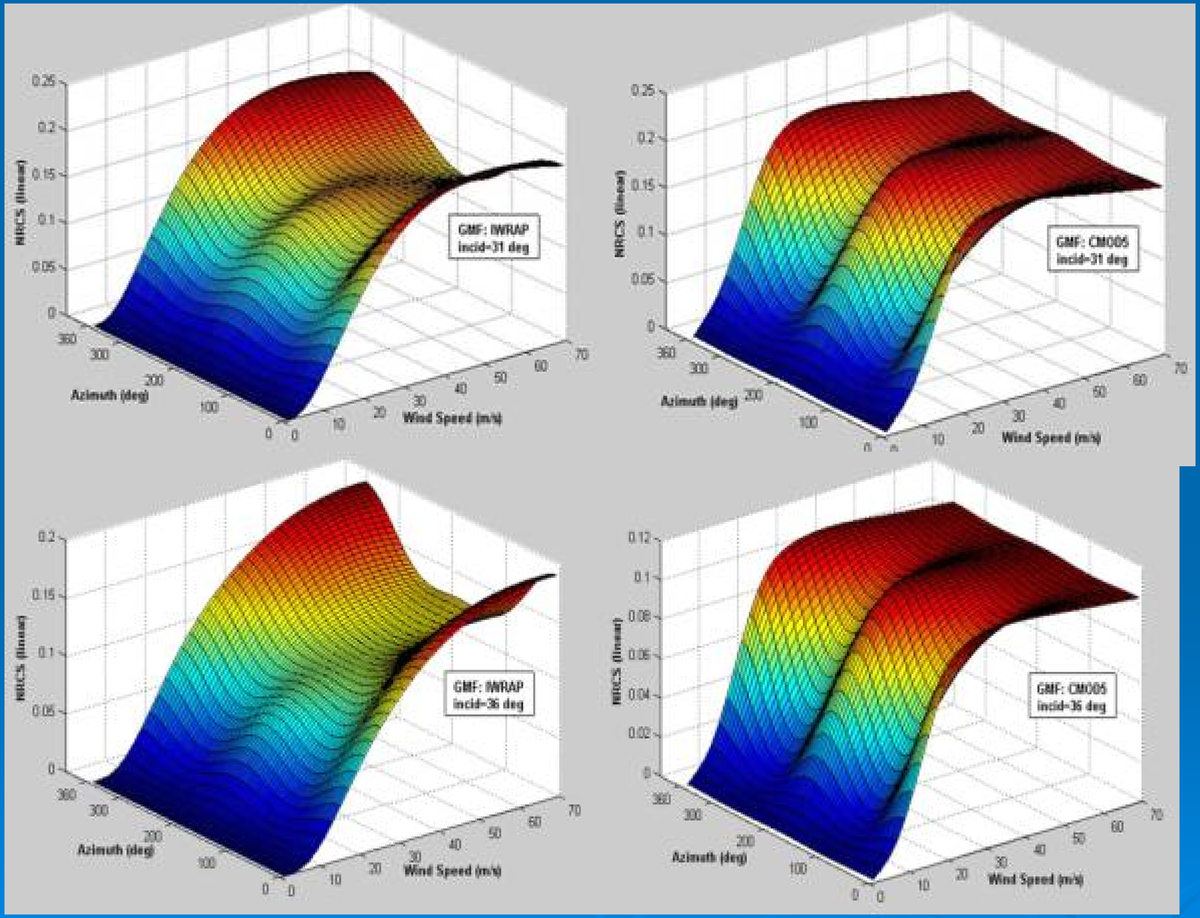

1) NRCS increases with wind speed;

2) Highest NRCS looking into the wind

3) Lowest NRCS looking cross wind;

4) A single NRCS measurement is not sufficient to infer wind speed;

5) NRCS saturates at high wind speed

6) CMOD5 and IWRAP GMF do not agree with each other in the high wind zone

3. SAR Hurricane Winds

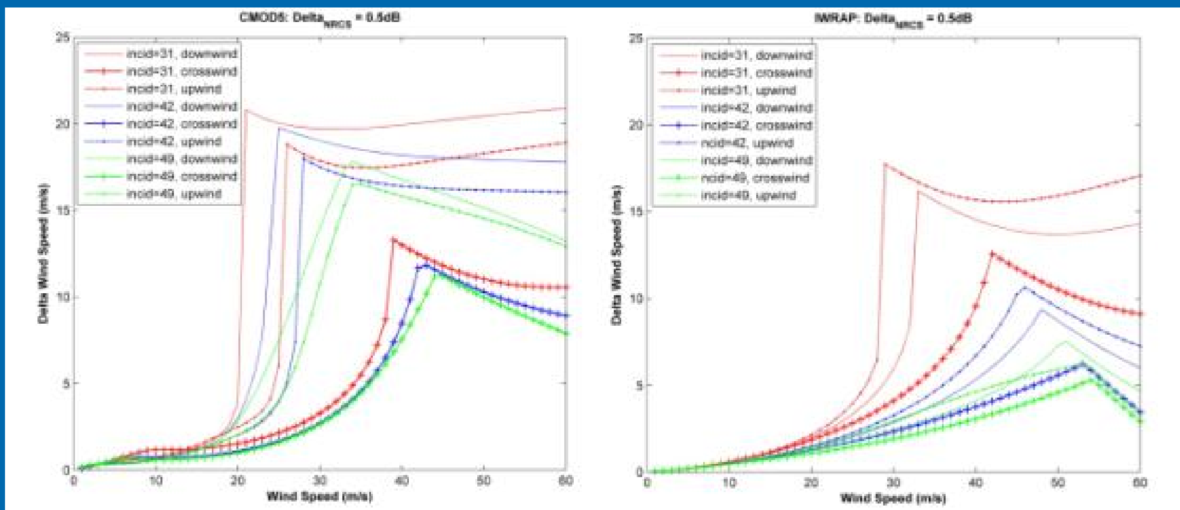

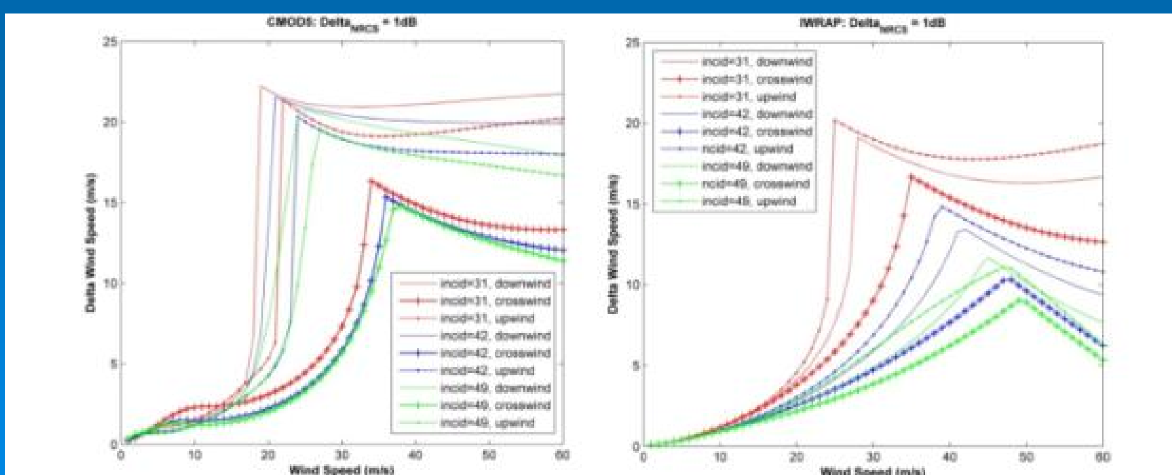

<u>Wind retrieval errors due to NRCS calibration errors</u>

(upper panel 0.5 dB,
Lower panel 1.0 dB)

Left panels are CMOD5
Right Panels are CIWRAP

3. SAR Hurricane Winds – Wind field reconstruction

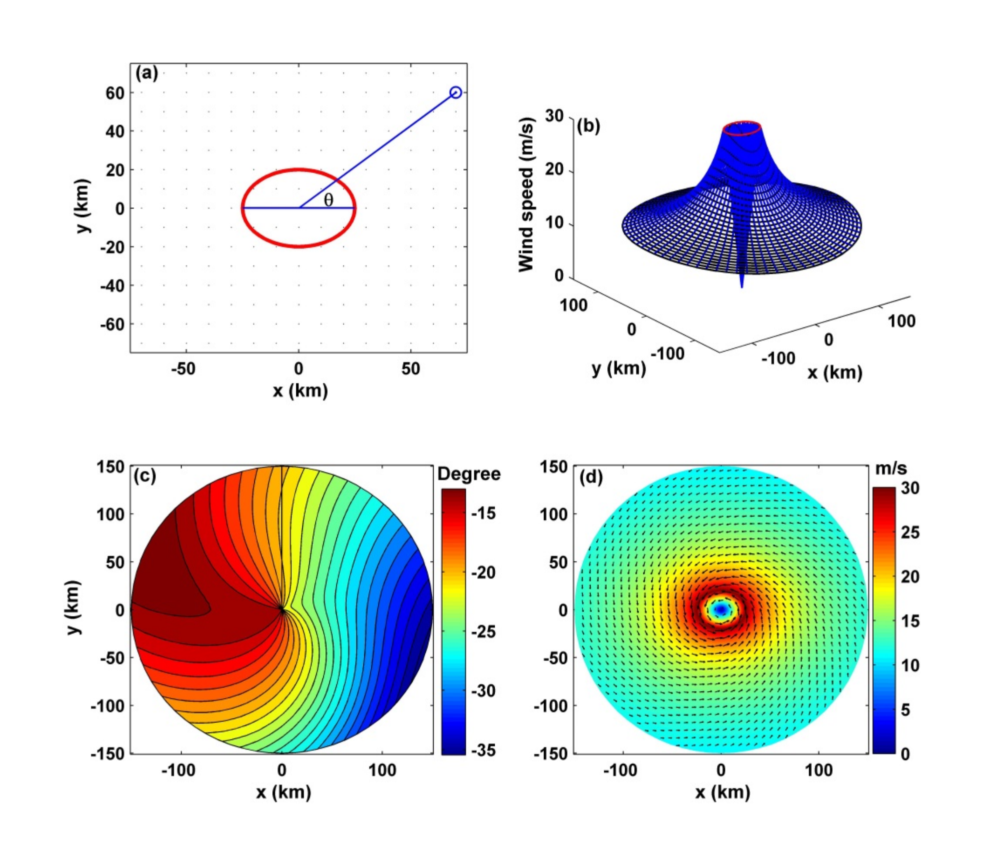

$a = 25\ km, b = 20km, V_{max} = 30\ m/s, \alpha = 0.5$

$$r_m(\theta) = a \cdot b / \sqrt{(b \cdot cos\theta)^2 + (a \cdot sin\theta)^2}$$

$$(r,\theta) = \begin{cases} V_{max} * \left[\dfrac{r}{r_m(\theta)}\right], & (r \le r_m(\theta)) \\ V_{max} * \left[\dfrac{r_m(\theta)}{r}\right]^{\alpha}, & (r_m(\theta) < r \le 150\text{ km}) \end{cases}$$

3. SAR Hurricane Winds – Wind field reconstruction

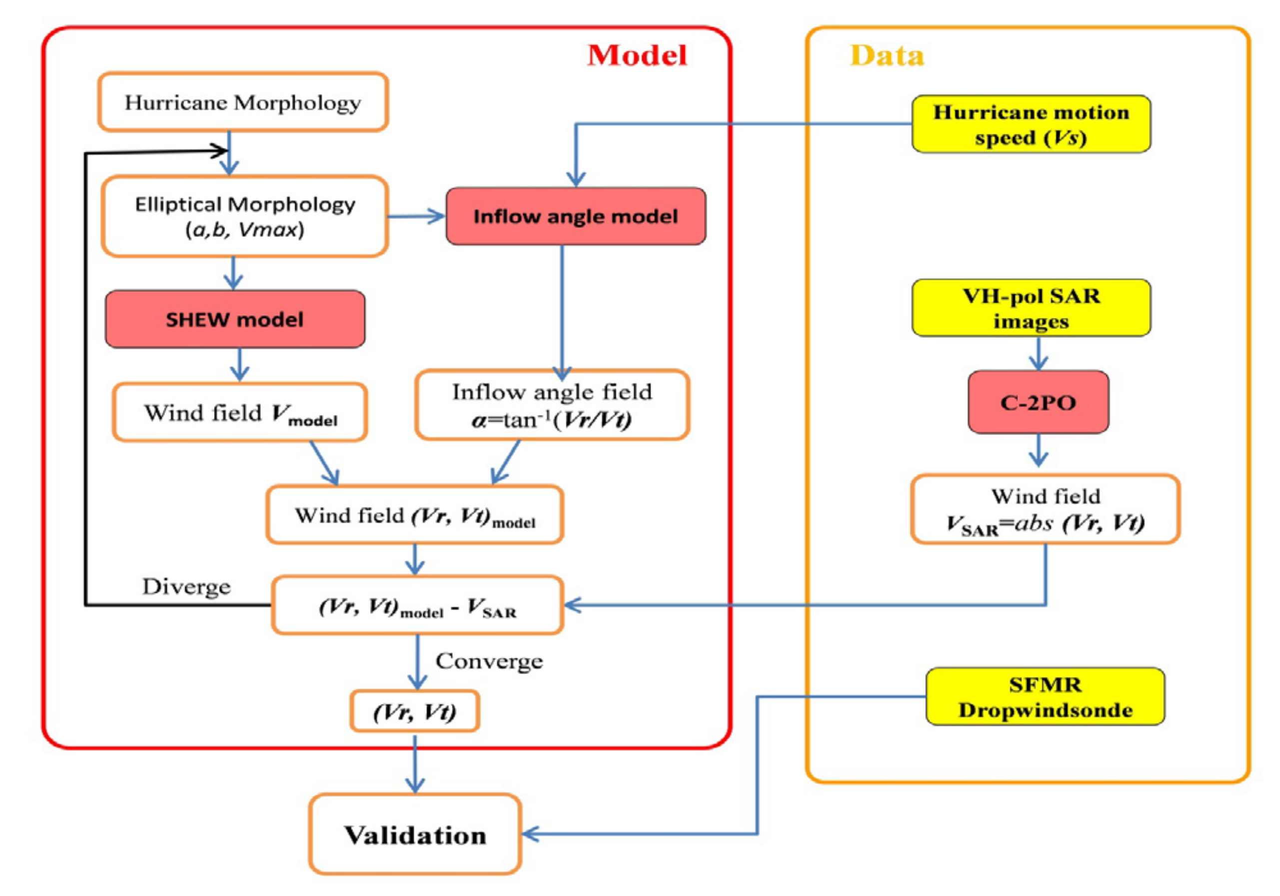

G. Zhang & X. Li et al., *IEEE TGRS*, *2016*

4. SAR Hurricane Winds

Hurricane Lane 18-August-2018

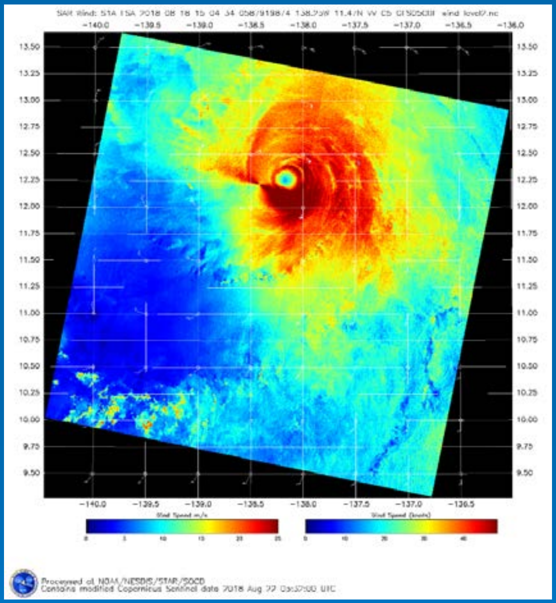

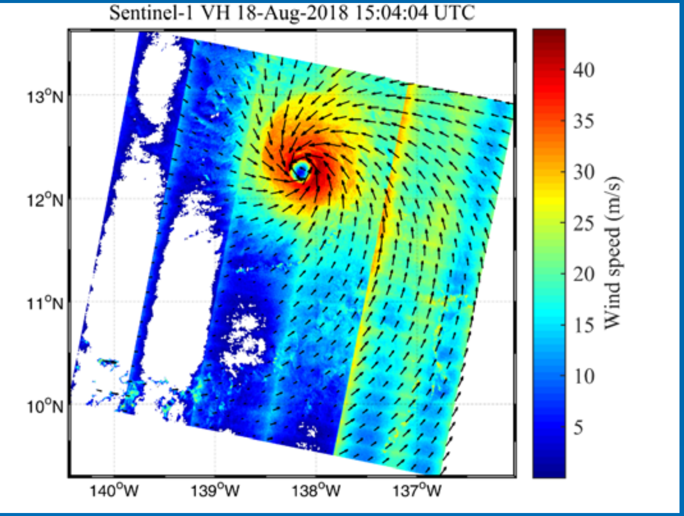

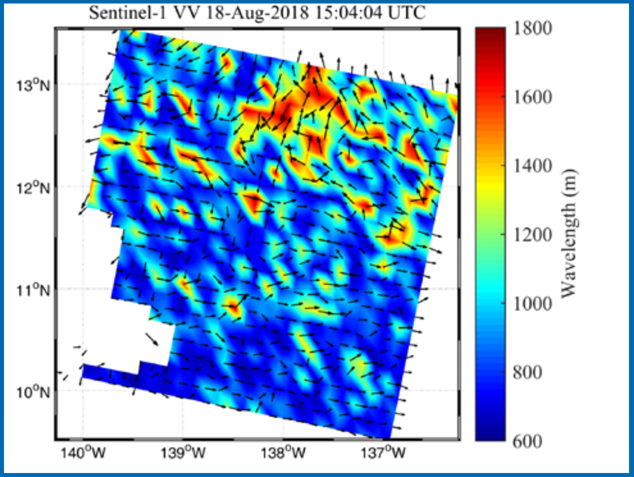

NOAA Wind

C3PO Cross-Pol +Inflow Angle Model
Pros: No Hour-Glass effect, no saturation, Wind Direction
Cons: beam scene boundaries

Boundary Layer Roll

4. SAR Hurricane Winds

Hurricane Lane 19-August-2018

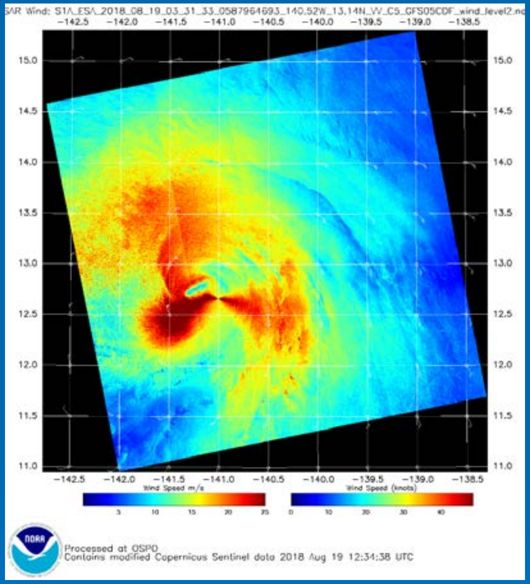

NOAA Wind

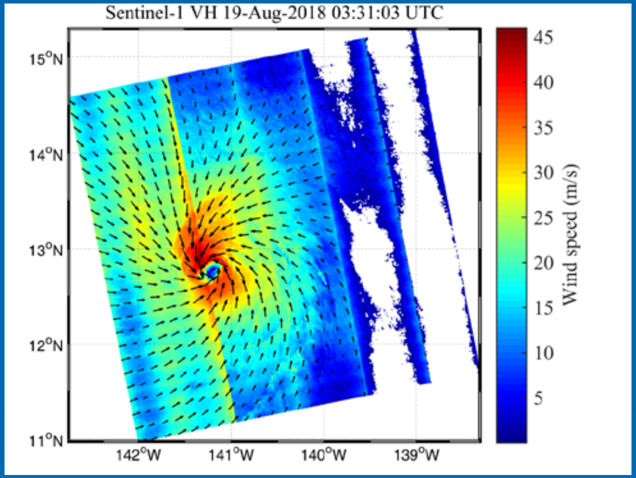

C3PO Cross-Pol +Inflow Angle Model

Pros: No Hour-Glass effect,

no saturation, Wind Direction

Cons: beam scene boundaries

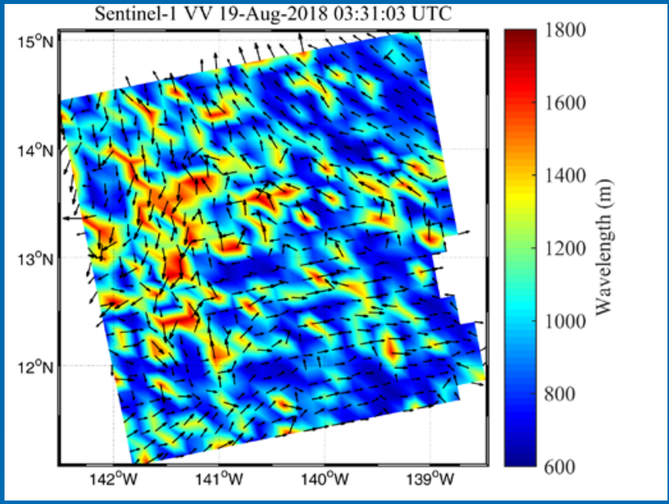

Boundary Layer Roll

4. SAR Hurricane Winds

Hurricane Lane 23-August-2018

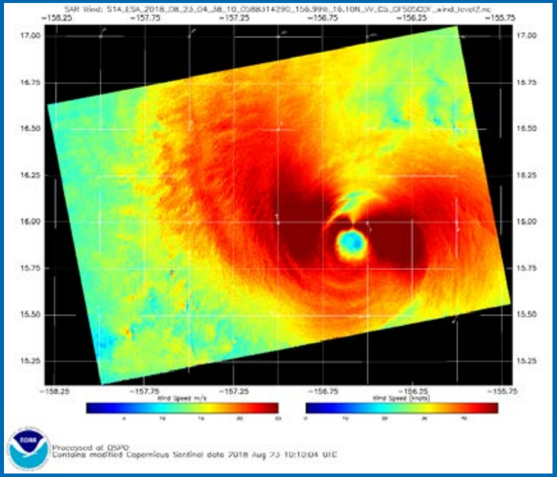

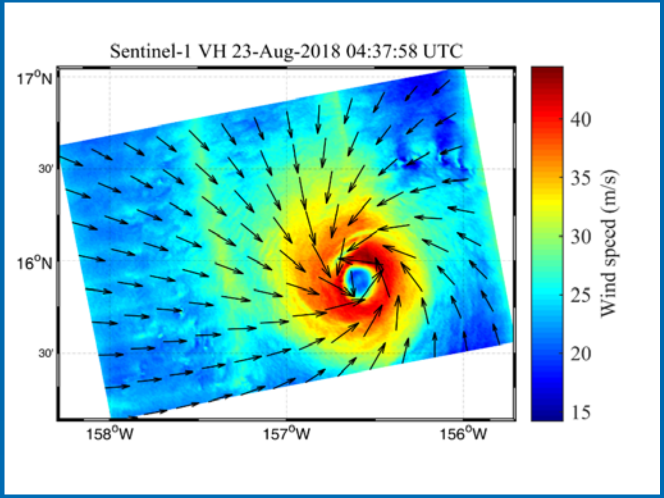

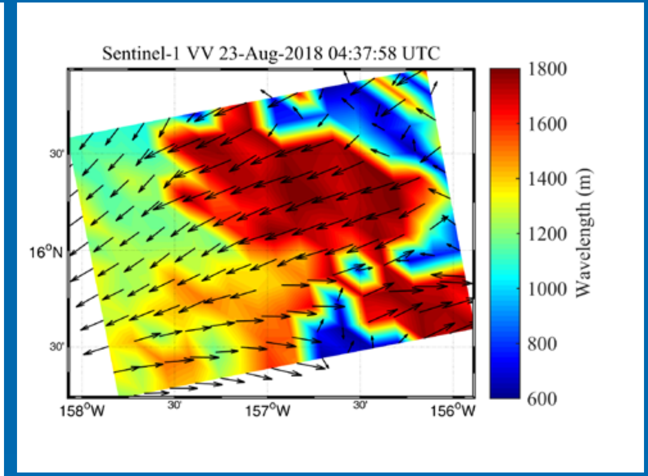

NOAA Wind

C3PO Cross-Pol +Inflow Angle Model
Pros: No Hour-Glass effect,
no saturation, Wind Direction
Cons: beam scene boundaries

Boundary Layer Roll

4. SAR Hurricane Winds

Validation - Hurricane Earl in 2010

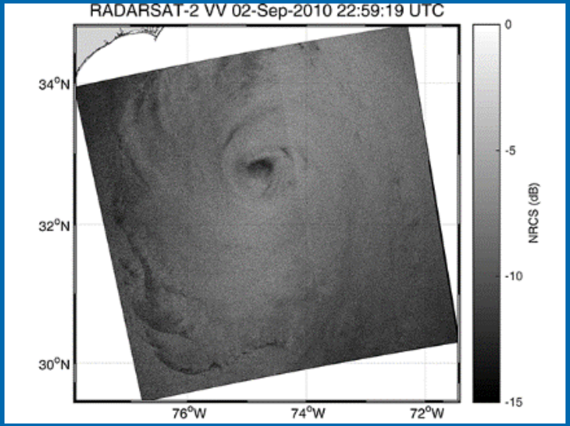

Hurricane Earl in 2010

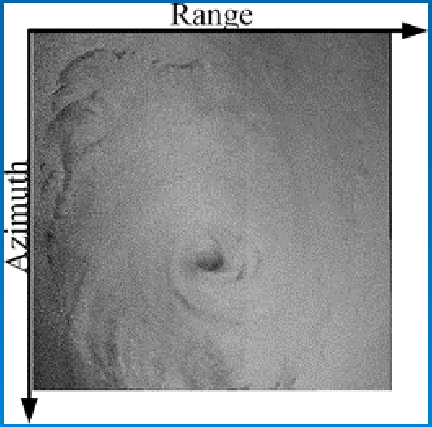

SAR VH polarization

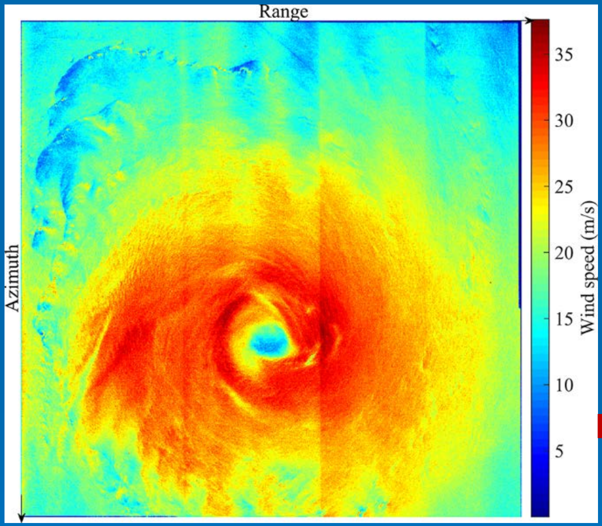

SAR wind field retrieval via C-3PO

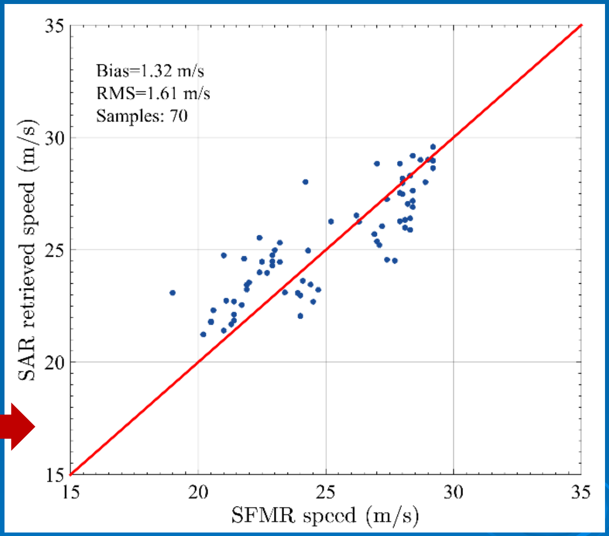

Validation: SAR retrieval vs SFMR

Zhang, G., X. Li, W. Perrie, P. A. Hwang, B. Zhang, and X. Yang (2017a), A hurricane wind speed retrieval model for C-band RADARSAT-2 cross-polarization scansar images, IEEE Transactions on Geoscience and Remote Sensing, 55(8), 4766–4774, doi:10.1109/TGRS.2017.2699622.

4. SAR Hurricane Winds – Wind field reconstruction

Research shows:

Mechanisms			VV-pol	VH-pol
Ocean surface	1. Microwave Diffraction on the craters produced by Rain		negligible	**important**
	2. Ring wave generated by Rain		**important**	**?**
	3. Damp to the wind wave induced by Rain		**important**	**?**
Atmosphere	4. Attenuation		negligible	**important**
	5. Volume backscattering		negligible	**important**

4. SAR Hurricane Winds – Wind field reconstruction

Three possible problem solved:

(1) SAR images capture incomplete hurricane core structures

(2) Radar signal is attenuated by the heavy precipitation associated with hurricanes;

(3) Wind directions retrievals are not available from the cross-polarized SAR.

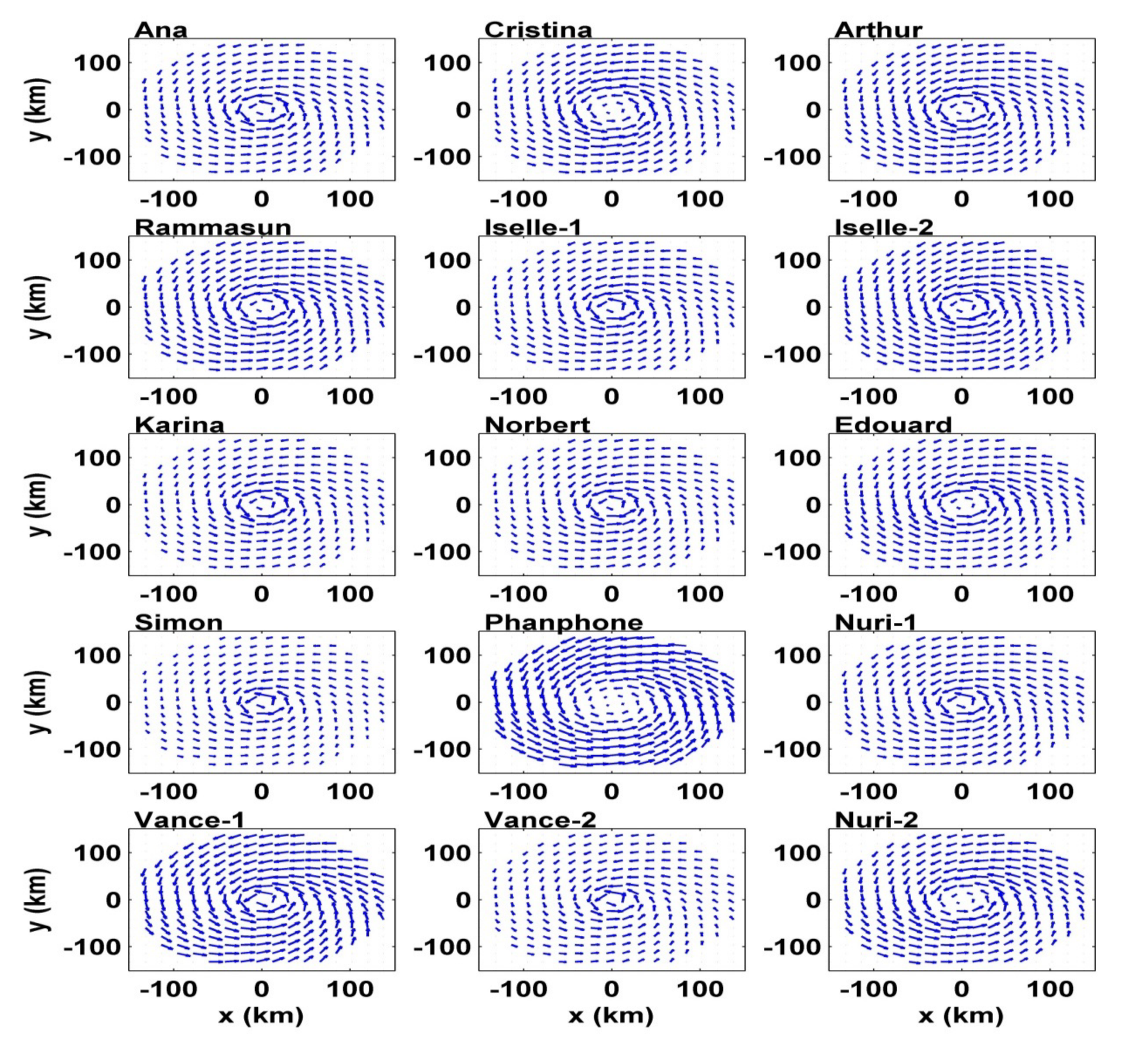

5 SAR Hurricane Waves

Wind retrieval errors due to NRCS Saturation
Solution 2: Wave Period- SWH – Wind triplet relationship

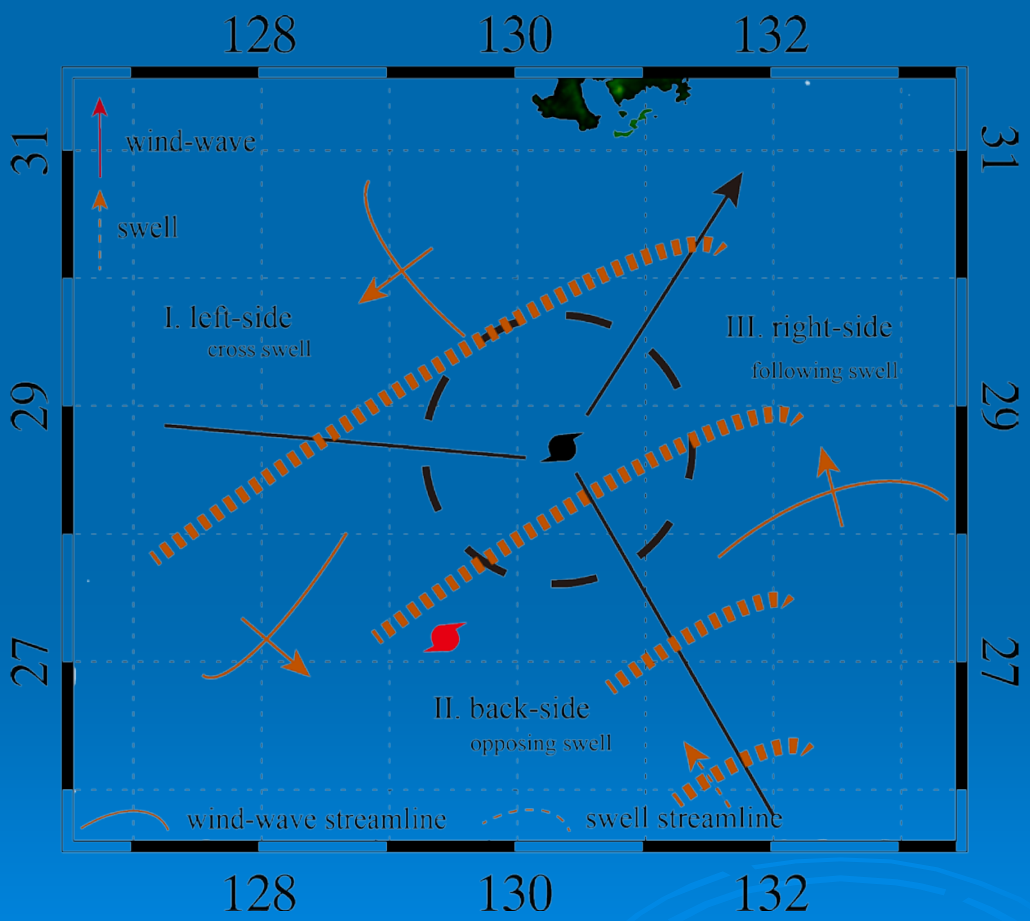

Wave Period- SWH – Wind triplet relationship

$$x_{\eta x}=\begin{cases}-0.26r+259.79, & \textit{right-side}\\ 1.25r+58.25, & \textit{left-side}\\ 0.71r+30.02, & \textit{back-side}\end{cases}$$

$$x_{\omega x}=\begin{cases}0.21r+170.0, & \textit{right-side}\\ 2.25r+24.85, & \textit{left-side}\\ 0.50r+14.16, & \textit{back-side}\end{cases}$$

$$U_{10}=397.46H_s^{0.841}x_{\eta x}^{-0.341}$$
$$U_{10}=91.49T_p^{1.900}x_{\omega x}^{-0.450}$$

Hwang et al., 2017 IEEE JSTARS

3. Hurricane forced wind

Wind retrieval errors due to NRCS Saturation

Solution 2: Wave Period- SWH – Wind triplet relationship

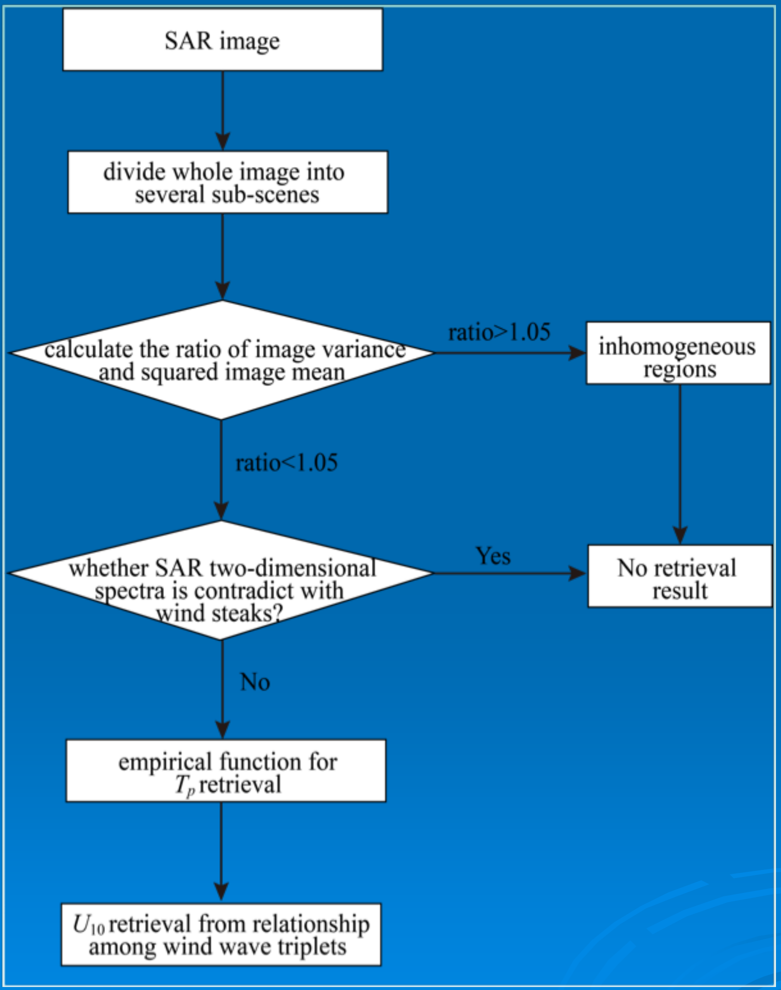

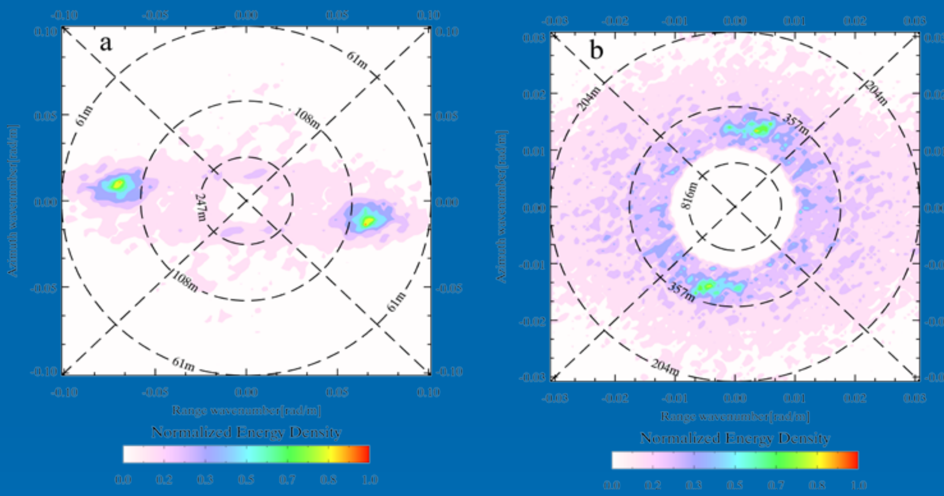

$$\lambda_{wave} = \lambda'_{SAR}(a - \theta_r / b)$$

$$\lambda'_{SAR} = \lambda_{SAR} / (\lambda_{SAR} / c)^d$$

Romeiser et al., [2015]

3. Hurricane forced wind

Wind retrieval errors due to NRCS Saturation
Solution 2: Wave Period- SWH – Wind triplet relationship

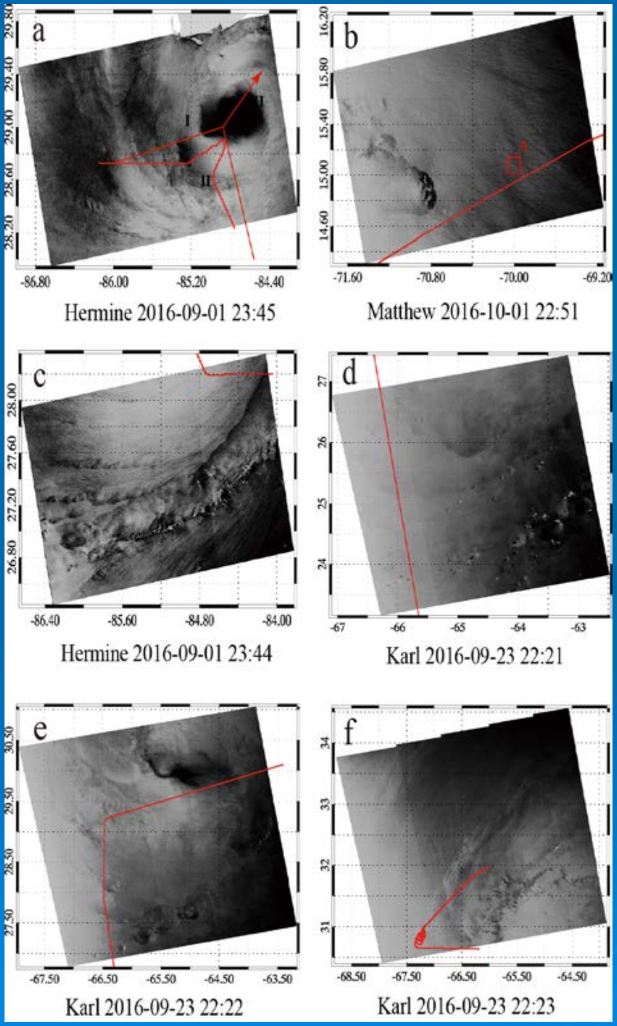

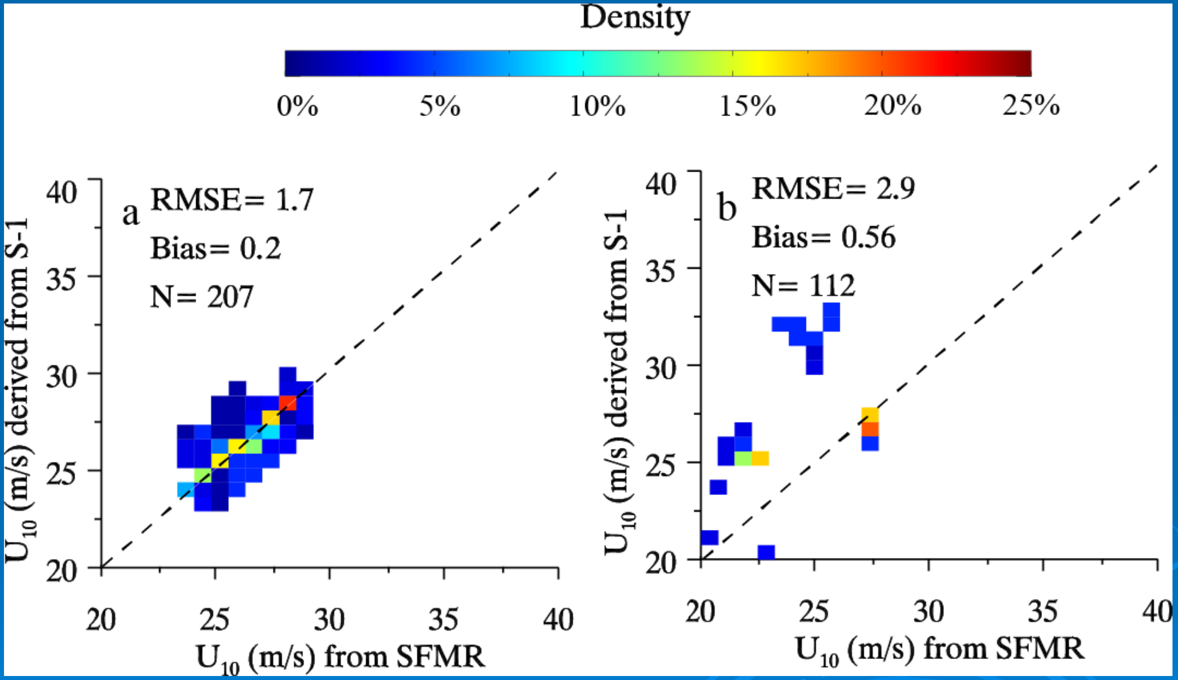

Sentinel-1 validation

Shao et al., 2017

5 SAR Hurricane Waves – Radarsat-2 Validation

Wind retrieval errors due to NRCS Saturation
Solution 2: Wave Period- SWH – Wind triplet relationship

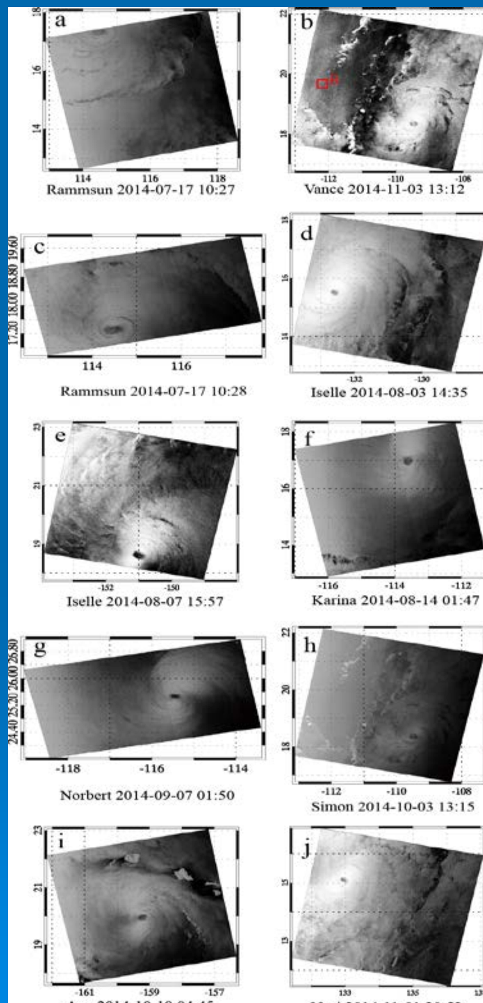

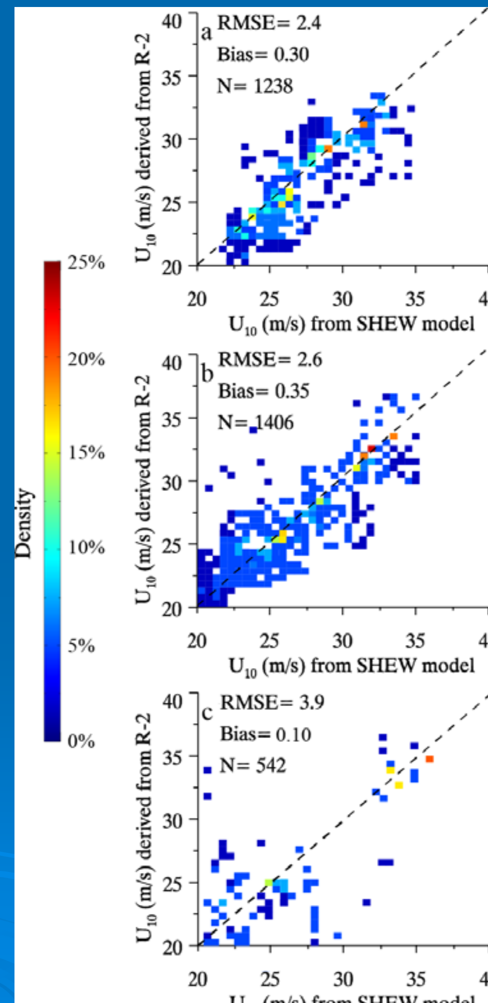

5 SAR Hurricane Waves – Sentinel-1 Validation

Three Sentinel-1 SAR images with SFMR observations
Hurricanes Hermine, Karl and Mattthew

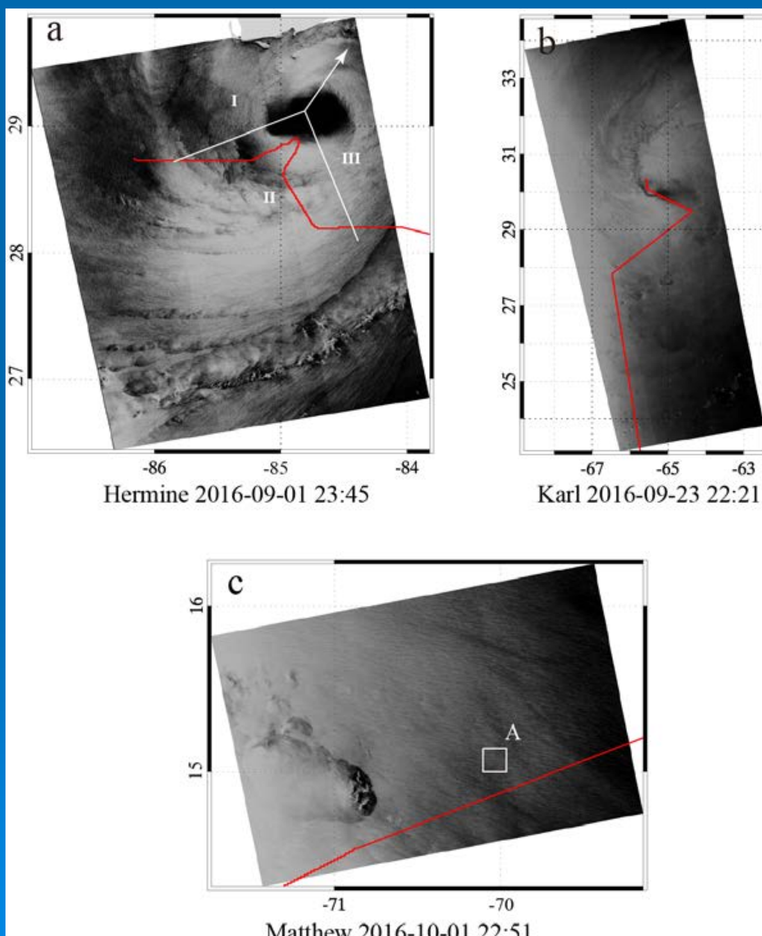

SAR spectrum of box A

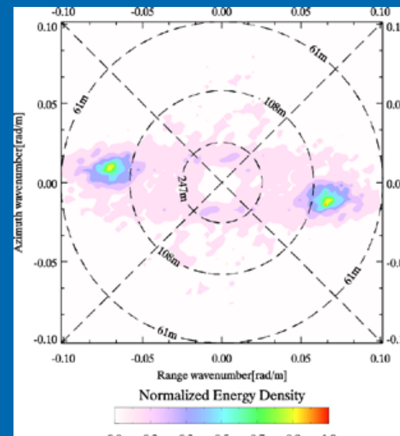

Wave Fetch in hurricane

$$U_{10}=91.49T_p^{1.9}x_{\omega x}^{-0.45}$$

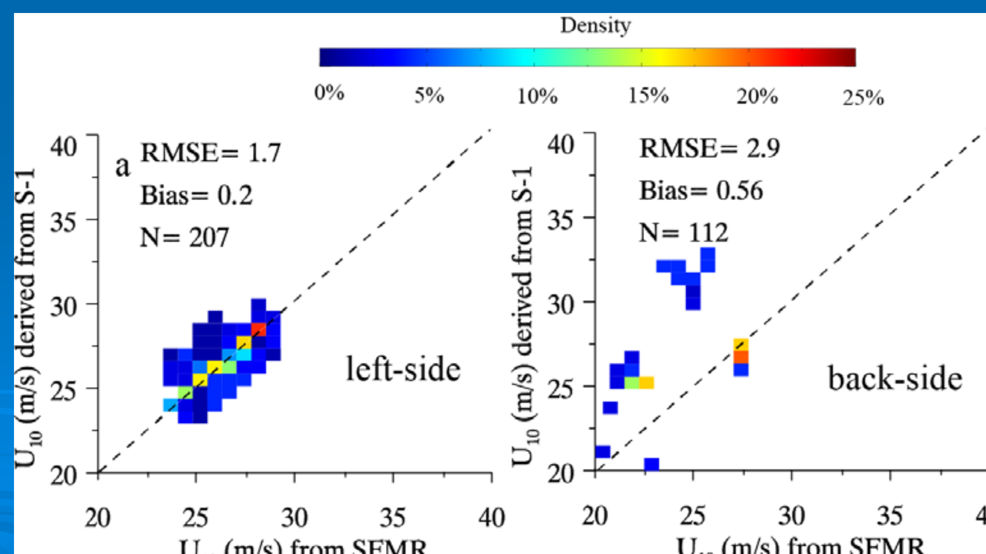

5 SAR Hurricane Waves

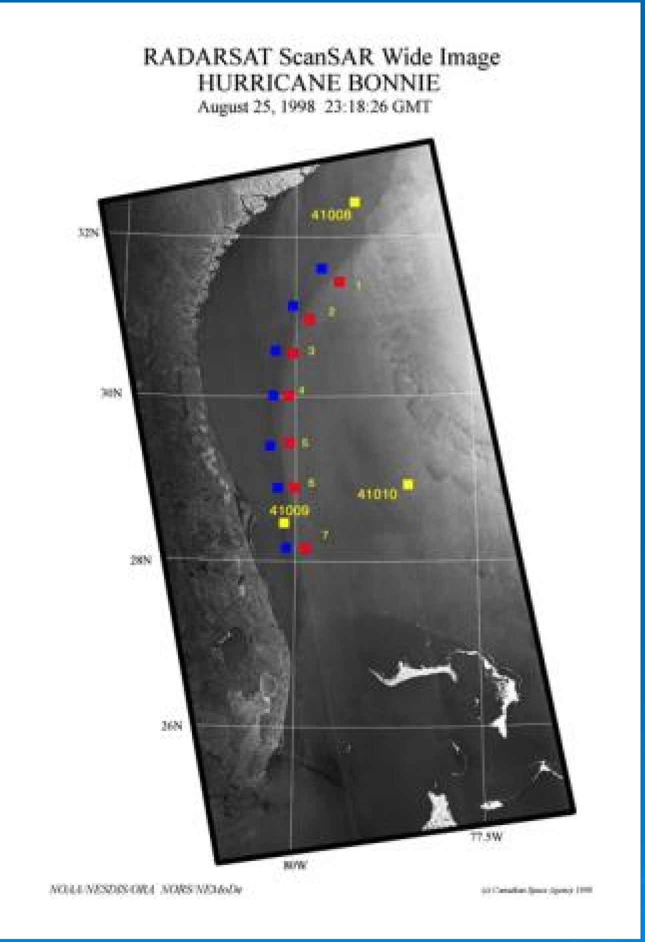

$$\sin(\theta_2) = \sin(\theta_1)\left[1 - \left(\frac{U}{C}\right)\sin(\theta_1)\right]^{-2}$$

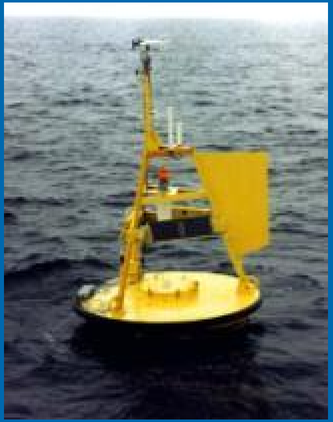

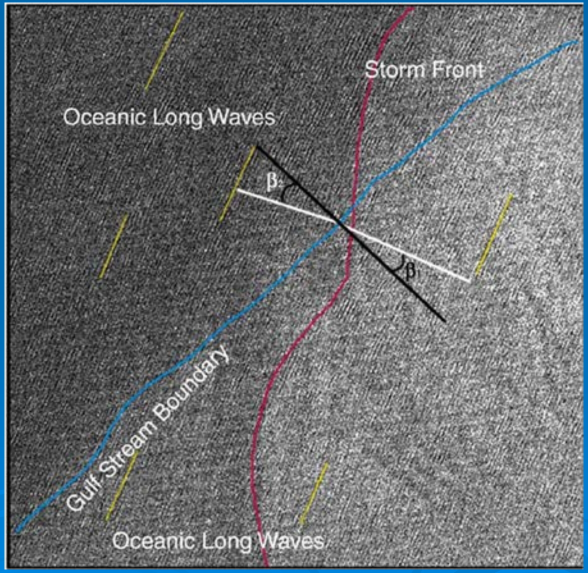

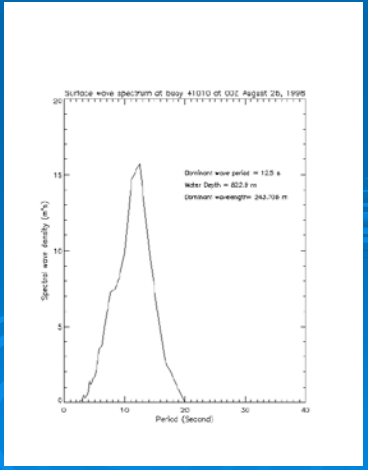

Li et al. IEEE-TGARS

5 SAR Hurricane Waves

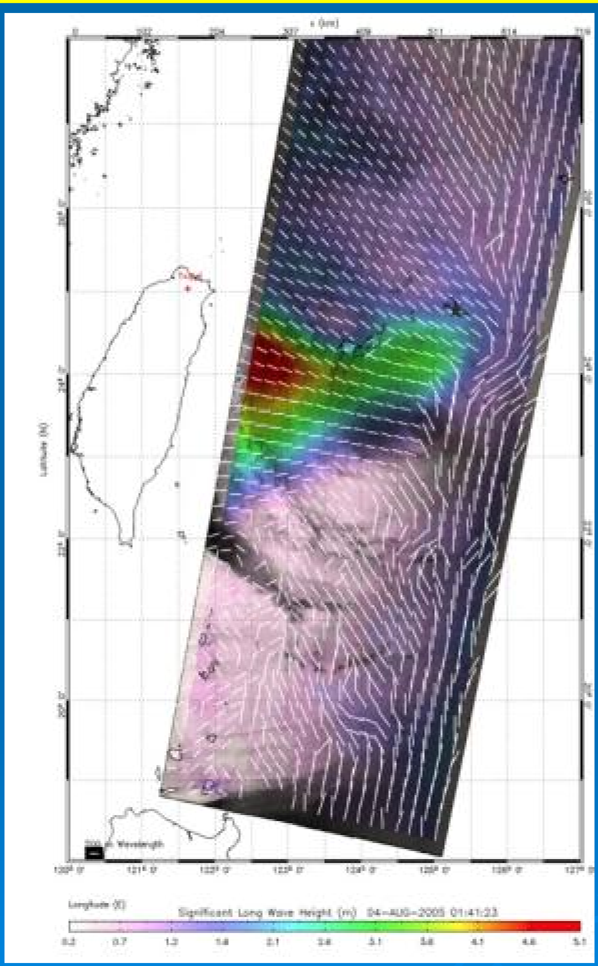

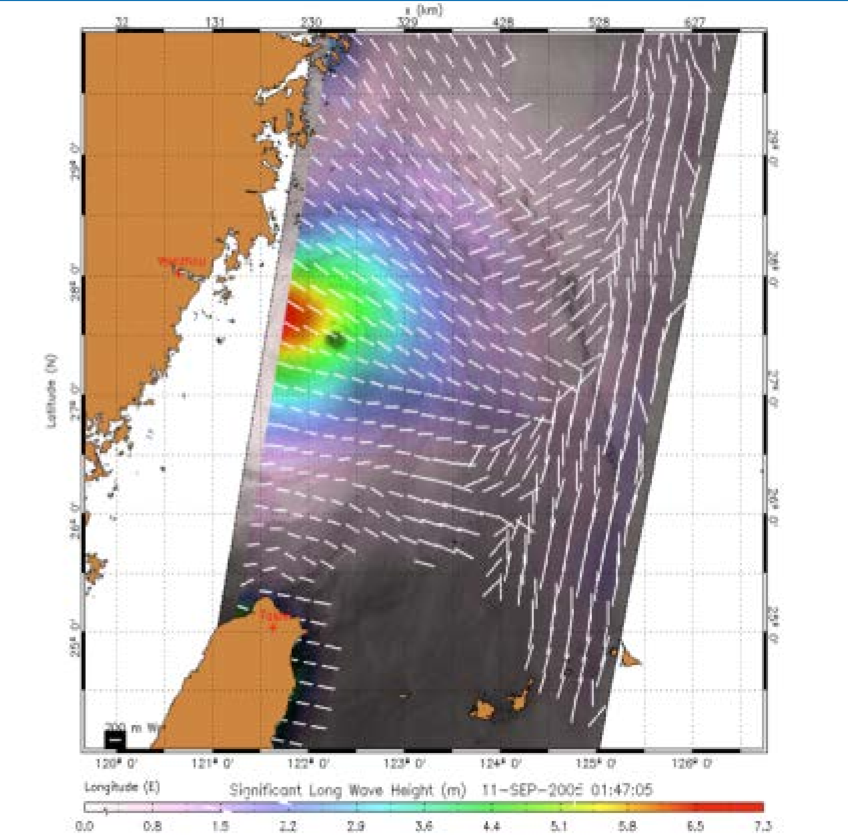

Significant wave height

4. SAR Hurricane Rain

On the ocean surface:

1. Microwave Diffraction on the craters produced by Rain
2. Ring wave generated by Rain
3. Damp to the wind wave induced by Rain

Transfer in the atmosphere:

4. Attenuation
5. Volume backscattering

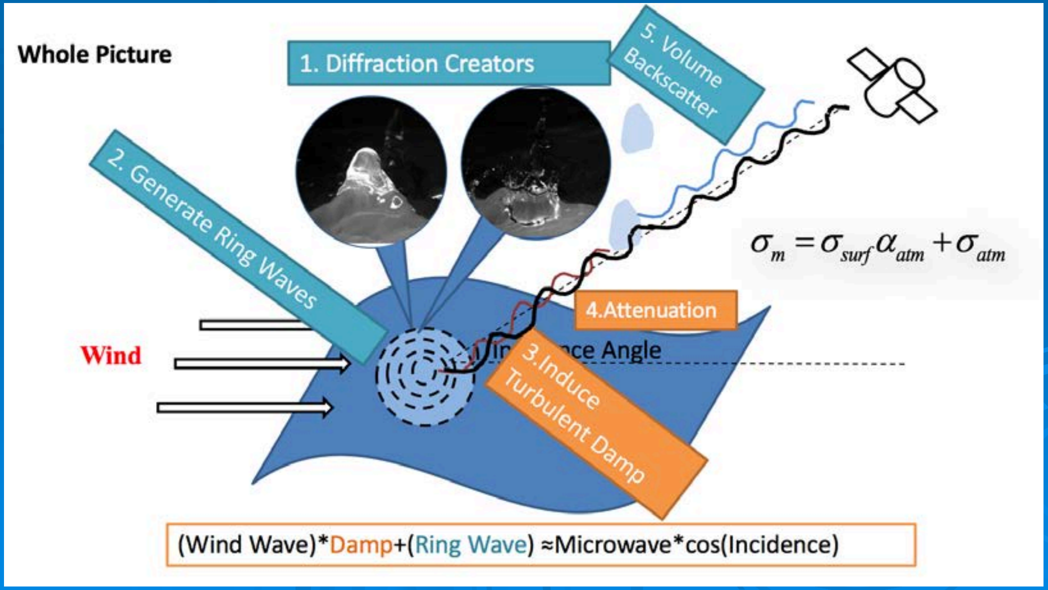

4. SAR Hurricane Rain

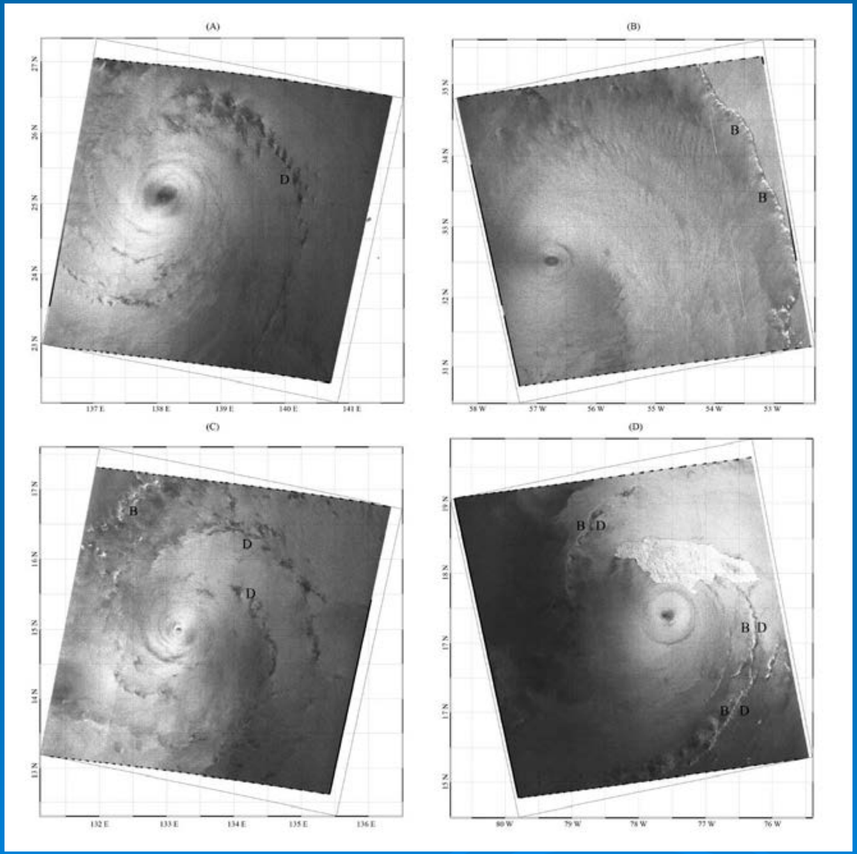

A and D also clearly reveal the signature of arc band of clouds (arc cloud).

Different rain band patterns observed in SAR images (All RADARSAT-1 images)
(A)Dark rain pattern; (B) Bright rain pattern; (C) Dark pattern in inner rain circle, and bright pattern in outer rain circle; (D) Bright-dark rain pattern in the same rain band.

4. SAR Hurricane Rain

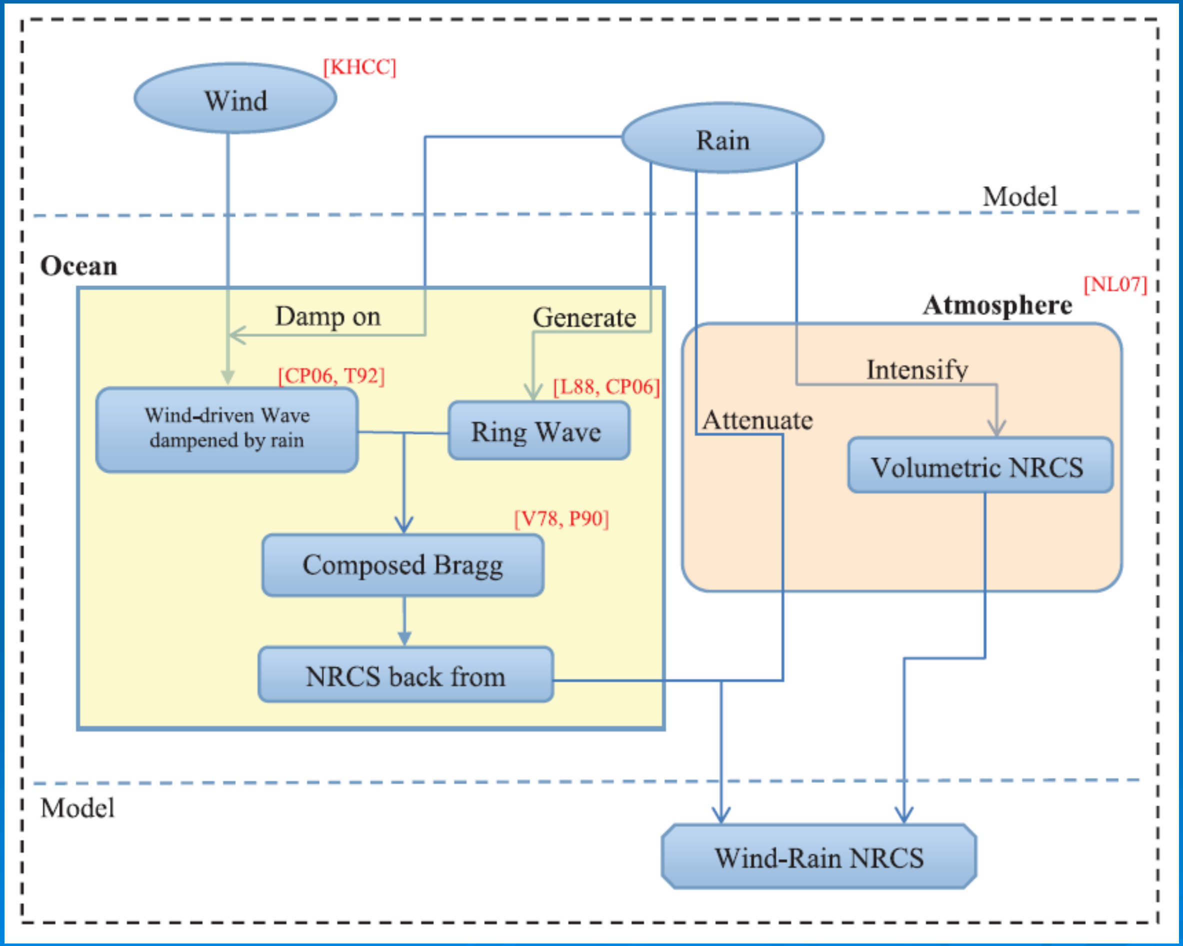

G. Zhang & X. Li et al., *JGR-Oceans*, *2015*

4. SAR Hurricane Rain

Blue line: Real track of the aircraft carrying SFMR
Cyan line: The track relative to hurricane center

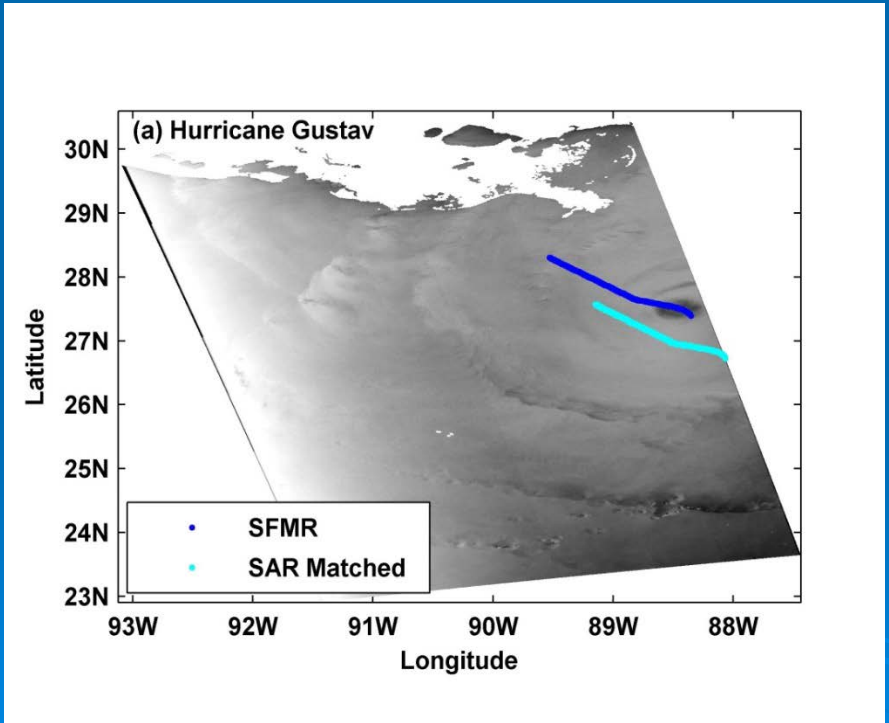

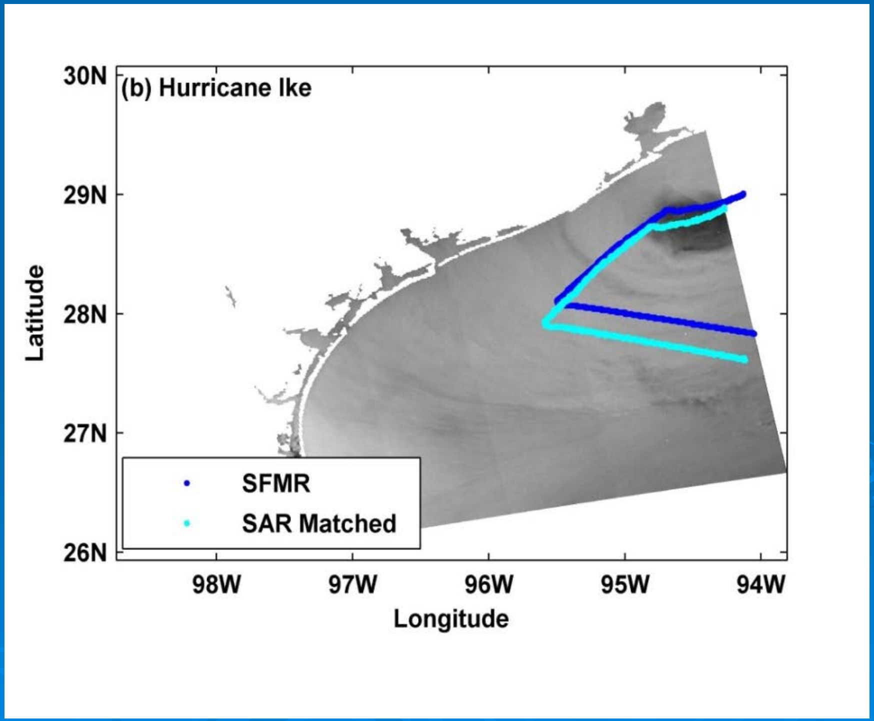

4. SAR Hurricane Rain Validation

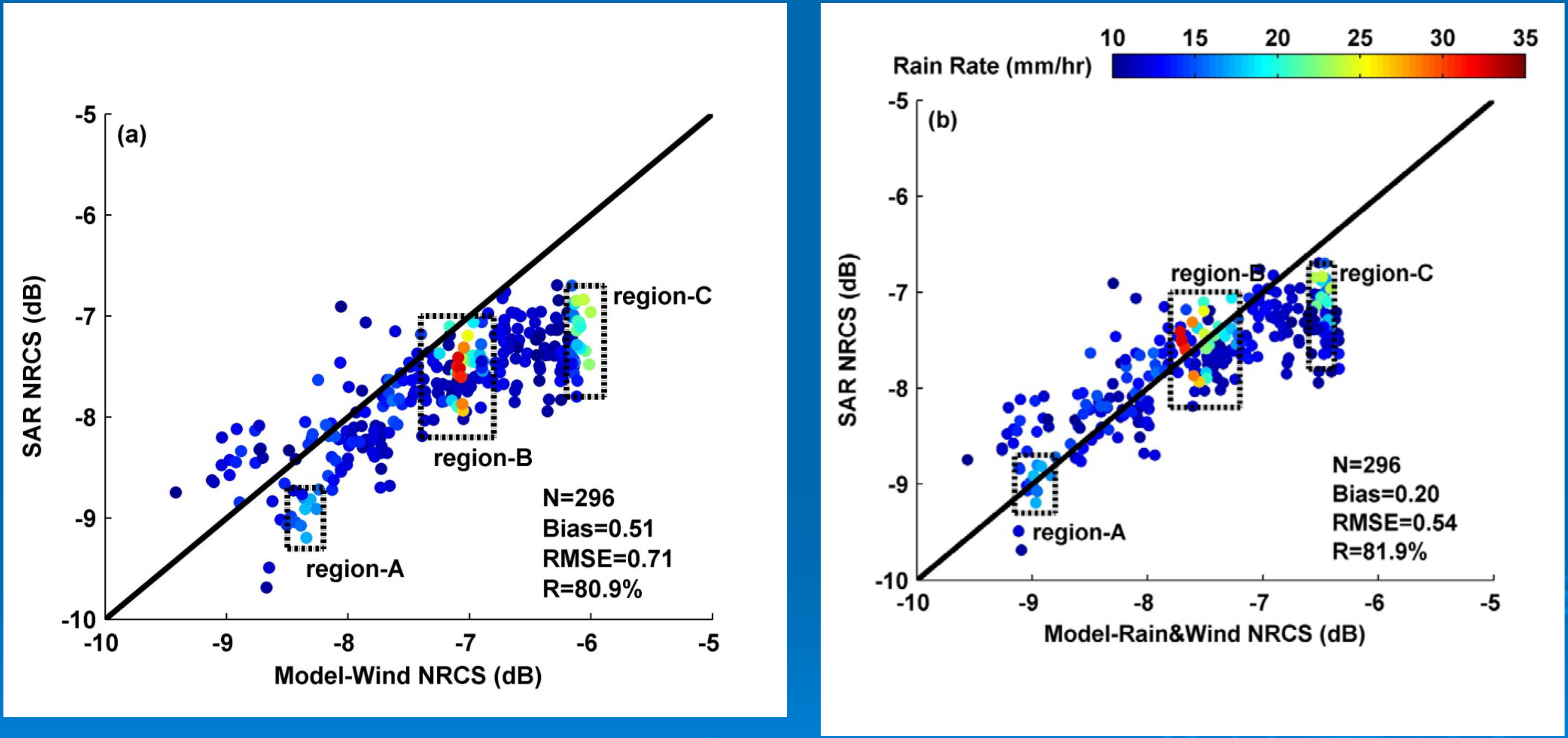

Comparisons between Simulated NRCS and ASAR observed NRCS

6 Summary

SAR wind data provides fine and detailed observation of sea surface imprints of hurricane structure:

- •Meso-votices
- •Rain bands and arc clouds
- •Boundary layer rolls
- •Storm patterns on land
- •High wind observed within certain tropical cyclone eyes

SAR surface wind analysis under extreme hurricane conditions underestimate the wind speed near the eye. Need further validation of SAR wind estimates, especially under very high wind speeds near hurricane eyes.

Hurricane eye information (shape and size) can be extracted from SAR images with image processing tools.

More analysis is under processing, such as hurricane precipitation, strong wind zone, and other hurricane characteristics.

6 Summary

1. SAR has wide applications in oceanic and atmospheric research
2. Some algorithms are mature enough to be implemented for operational use
3. ESA Sentinel-1 was launched
4. There will be CSA RADARSAT-C SAR data available in the 2014-2016. For the first time, SAR data policy will be free and open

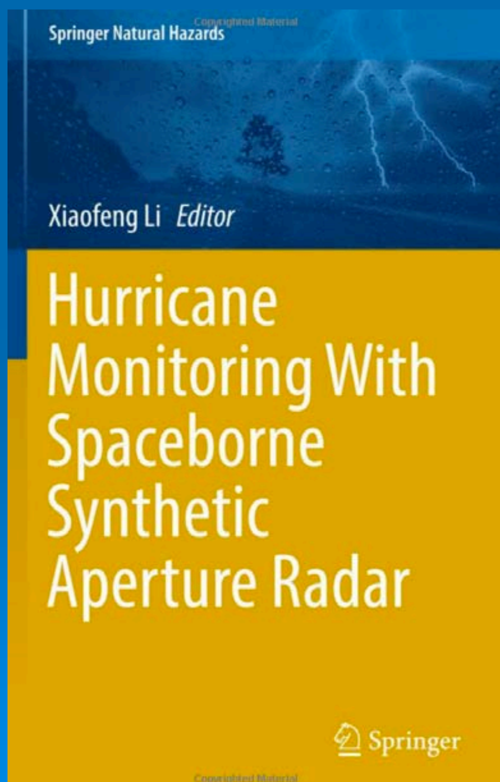

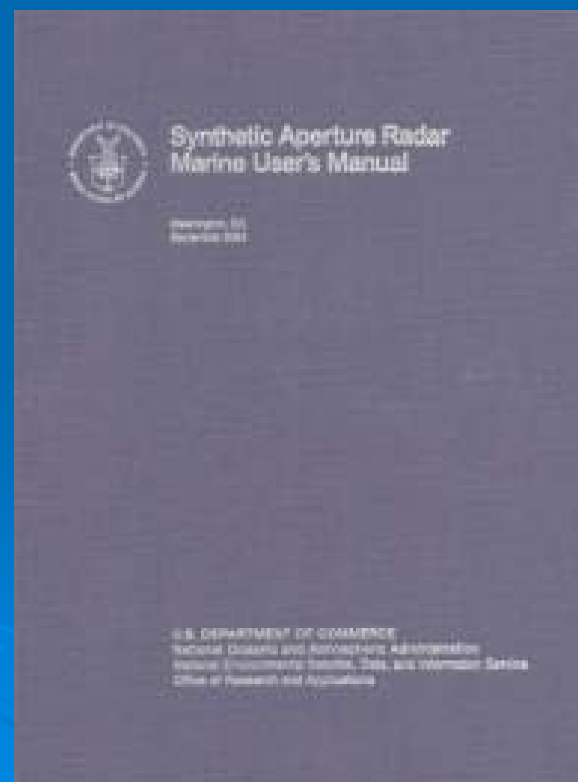

References

Hurricane Wind:

- Zhang, G. S., W. Perrie, X. Li*, and J. A. Zhang (2017), A Hurricane morphology and surface wind vector estimation model for C-band cross-polarization SAR, IEEE Trans. Geosci. Remote Sens., doi: 10.1109/TGRS.2016.2631663.
- Zhang, G., X. Li*, W. Perrie, P. Hwang, B. Zhang and X. Yang (2017), A hurricane wind speed retrieval model for C-band Radarsat-2 cross-polarization ScanSAR images, IEEE Trans. Geosci. Remote Sens., VOL. 55, NO. 8, 4766- 4774, doi: 10.1109/TGRS.2017.2699622.

Wave:

- Shao, W., X. Li*, P. Hwang and B. Zhang, X. Yang (2017), Bridging the gap between cyclone wind and wave by C-band SAR, J. Geophys. Res. Oceans, doi: 10.1002/2017JC012908.
- Li, X.*, W. Pichel, M. He, S. Wu, K. Friedman, P. Clemente-Colon, C. Zhao, Observation of Hurricane-Generated Ocean Swell Refraction at the Gulf Stream North Wall with the RADARSAT-1 Synthetic Aperture Radar, IEEE Trans. Geosci. Remote Sens., Vol. 40, No. 10, 2131-2142, doi: 10.1109/TGRS.2002.802474, 2002.

Boundary Layer Rolls:

- Huang, L., X. Li*, B. Liu, J. A. Zhang, D. Shen, Z. Zhang, W. Yu (2018), Tropical Cyclone Boundary Layer Rolls in Synthetic Aperture Radar Imagery, J. Geophys. Res. Oceans, DOI: 10.1029/2018JC013755..

Hurricane Morphology:

- Li, X.* (2015), The First Sentinel-1 SAR Image of a Typhoon, Acta Oceanol. Sin., 34(1): 1-2, doi: 10.1007/s13131- 015-0589-8.
- Jin, S, X. Li*, S. X. Yang, J. Zhang and D. Shen (2017), Identification of tropical cyclone centers in SAR imagery based on template matching and particle swarm optimization algorithms, DOI: 10.1109/TGRS.2018.2863259.
- Jin, S., S. Wang, X. Li, L. Jiao, J. A. Zhang and D. Shen (2017), Center location of tropical cyclones without eyes in SAR images based on salient region detection and pattern matching, IEEE Trans. Geosci. Remote Sens., Vol. 55, No. 1, 280-291, doi: 10.1109/TGRS.2016.2605766.
- Lee, I., A. Shamsoddini, X. Li*, J. C. Trinder, Z. Li (2016), Extracting hurricane eye morphology from spaceborne SAR images using morphological analysis, ISPRS J. Photogramm. Remote Sens., Vol. 7, 115-125, doi: 10.1016/j.isprsjprs.2016.03.020.
- Li, X.*, J. A. Zhang, X. Yang, W. G. Pichel, M. DeMaria, D. Long, and Z. Li (2012), Tropical cyclone morphology from spaceborne synthetic aperture radar, Bull. Amer. Meteorol. Soc., doi:10.1175/BAMS-D-11-00211.1.

Hurricane Rain:

- Zhang, G. S., X. Li*, W. Perrie, B. Zhang, and L. Wang (2015), Rain effects on the hurricane observations over the ocean by C-band Synthetic Aperture Radar, J. Geophys. Res. Oceans, 120, doi:10.1002/2015JC011044. PDF
- Xu, F., X. Li, P. Wang, J, Yang, W. Pichel and Y-Q Jin (2015), A backscattering model of rainfall over rough sea surface for synthetic aperture radar, IEEE Trans. Geosci. Remote Sens.. doi: 10.1109/TGRS.2014.2367654.

Thank you!

xiaofeng.li@noaa.gov